VOLUME 3

INNOVATION

A STUDENT RESEARCH JOURNAL

PUBLISHED BY STEMY

Contents

Authors

Naren Alluri, Shireesh Kumar, Lokesh Nanthakumar

Smrithi Balasubramanian, Sreevatsa Vemuri

Jane Hu, Ellie Hummel

Dharshini Kumar

Anna Morgan

Editor-in-Chief

Bhavana Pavuluri

Editors

STEMY *Innovation* Team

Graphic Design

Marjorie Mays

Letter From the Editors

We are STEMY (STEM + Youth), a local, student-run nonprofit on a mission to break gender, racial, and socioeconomic barriers through science, technology, engineering, and math (STEM) education. Through our programs, we aim to spark passions for STEM among disadvantaged and underrepresented students.

STEMY began as an after-school club called the Manual Science Review (MSR), which aimed specifically to help duPont Manual High School students with their science fair projects. After about a year, we saw the tangible impacts that the MSR's programs had on the school—program participants came to enjoy the scientific research process and grew more interested in STEM—and we wanted to expand beyond just our high school. Officially founded about three years ago, this organization is the result of our drive to change lives by engaging all students, regardless of gender or background, in STEM. We have already directly impacted well over 1,000 local students from all backgrounds and plan to engage thousands more in new programs.

Effective STEM education is not just valuable to improve academic performance—the right kind of learning influences students' career options, worldview, and mindset. High-quality STEM experiences have been shown to improve problem-solving skills, build confidence, and motivate students to enter high-paying jobs in the future. STEM programs like ours lead participants to view the world through an observation-based, curiosity-driven lens and have the power to open minds that have been closed by years of learning through rote memorization. Critically, sparking passions for STEM among underrepresented and disadvantaged students can break down established social barriers in STEM fields.

Our initiatives aim to engage students in exciting, creative STEM activities to build new skills and spark new passions among participants. *Innovation* is one of these many programs. All across this city, there are talented, dedicated high school students who pursue incredible research projects and demonstrate the amazing things students with strong STEM backgrounds can do. We believe that these students deserve the opportunity to showcase their efforts, which is why we created *Innovation*.

Innovation, just like our organization, is created and produced by students and students only. We cultivate strong partnerships among editors and authors and give writers the unique opportunity to publish high-quality, peer-reviewed work as a high schooler. Through this journal, we hope to spread the innovative spirits of our authors and their amazing research throughout the community. We believe that *Innovation* is a unique way to expose Louisville to STEM, and we will continue to produce and publish this journal for years to come.

A Low-Cost Prosthetic Arm Controlled by Muscle Sensors

Naren Alluri[1], Shireesh Kumar[1], Lokesh Nanthakumar[1]
[1]duPont Manual High School
Louisville, Kentucky

ABSTRACT

There are over 185,000 amputations in the United States each year ("Amputee Statistics," n.d.) with the average cost of a prosthetic ranging from $5,000 to $50,000 (Mohney, 2013). Many expensive prosthetics require patients to alter their neural connections to receive optimal functioning in their amputation. As a result, a prosthetic arm controlled by muscle sensors was created. It was a three-step process. First, the arm was created using CAD software and was then converted into a Makerbot system, which printed out the arm in polylactic acid. The second step was creating a program from Arduino that created six movements of the arm: all fingers open and close, two fingers open and close, and one finger opens and closes. The final step was connecting the muscle sensor to the arm. There were four main pieces: electrodes, muscle sensor, servo, and the breadboard.

The arm was tested by 50 participants. The participants decided where to put the muscle sensors on their bodies. Out of 50 patients, 23 placed their sensors on their calf, 13 placed their sensors on their shoulders, 7 placed their sensors on their backs, and 7 placed their sensors on their foreheads. The six different programs were run for each participant, and there was a total accuracy of 96.2 percent.

INTRODUCTION

There are millions of prosthetic limbs around the globe, with a new one created every 30 seconds. A prosthesis is an artificial limb that is used to replace limbs that have been amputated due to war, accidents, or illnesses. There are four parts to a prosthesis: the socket, the prosthetic limb, the control system, and the attachment mechanism (Woodford, 2010). Each of these parts works with the others to create an effective prosthetic apparatus.

The purpose of this project is to create an affordable prosthetic arm that is controlled by muscle sensors. Current prosthetics require alterations of nerve pathways for the arm to have optimal functioning. The societal impact of the prosthetic arm described in this project is that war veterans and others alike will be able to have a replacement leg that is controlled similarly to a regular leg without paying more money. This project aims to test whether the connection of a MyoWare muscle sensor will contribute to the functions of the prosthetic arm. Therefore, this project's engineering goal is to create a successful working prototype of a muscle-controlled prosthetic arm.

In a study by Shriya Srinivasan, a graduate student in the Harvard-MIT Program in Health Sciences and Technology, she demonstrated in rats a technique that generates muscle-tendon sensory feedback to the nervous system, which conveys information about a prosthetic limb placement and the forces applied to it (MIT, 2017). This study connects to the hypothesis because the same technique can also be applied to humans due to the various nerves that connect the limbs to the brain. For humans with prosthetics, the muscles are severed in a way that cuts off a key relationship that normally helps people control their limbs and sense where they are in space. Most muscles that control limb movement occur in pairs known as agonist-antagonist pairs, which are characterized by one muscle stretching when the other is contracting. For example, when an elbow bends, the biceps muscle contracts, causing the triceps to stretch. That stretch of the triceps sends sensory information related to position, velocity, and force back to the brain. Using sensors for people with prosthetics will produce the relationship that allows people to control position and stiffness at their limb joints.

In another study conducted by Professor Andrew Schwartz and various other accredited scientists from the University of Pittsburgh, electrodes were wired into the brains of two monkeys, each of whom had one of their arms amputated (Carey, 2008). A prosthetic arm was

attached to the amputated part of each monkey, connecting the prosthetics to the sensors in the monkeys' brains. After multiple attempts, these monkeys learned how to use their thoughts to control the prosthetic arm by learning how to grab food, adjust the size of morsels, and more (Carey, 2008). This study aims to apply this same scenario to humans. In monkeys, the brain's motor cortex, which sends neural messages to the limbs/muscles of the body, is not as sophisticated as that of humans. Therefore, when applying brain-controlled prosthetics to humans, the highly sophisticated motor cortex needs to be accounted for. Furthermore, the tasks performed by the monkeys in the study above were relatively simple, indicating that the prosthetic itself was not very sophisticated.

METHODOLOGY

In order to create and plan the project, a three-step process was developed. The first step was the creation of the arm. To do this, a sketch of the prosthetic arm was drawn on graph paper using a convenient scale to estimate the amount of material needed. This design was then modeled digitally using CAD (Computer-Aided Design). Afterwards, the arm was printed using a MakerBot 3D printer in four separate parts: the fingers, the hand, the bicep, and the forearm. The parts were then glued together using polylactic acid.

The second step of the process was connecting the muscle sensor to the arm. A MyoWare muscle sensor (EMG), an Arduino Pro Mini Board, two servo motors, a breadboard, solder, wires, and electrodes were purchased. First, the Arduino board was placed onto the breadboard. The breadboard receives the code from the computer and transports the information to the EMG sensor. It was important to place the Arduino board on the breadboard because it contains the USB slot that allows the computer to be connected to the breadboard. Then, the EMG Sensor was connected to the end of the breadboard, corresponding to the Arduino board. With another wire, the signal end of the EMG Board was connected to the other end of the breadboard, corresponding to the Arduino board. This wire allows the information read on the sensor to be sent back to the computer so that it can process the code. Next, the servo motor was connected to the breadboard. The servo motor is the item that actually causes the movement of the arm, so by connecting it to the breadboard, it will be able to follow the code on the computer.

The next step was to program the connection of the arm to the muscle sensor. The program was created in Arduino. Variables were created to initialize the parts of the sensors, such as the EMG sensor and the servo motor. Also, a threshold was created, and it represents the number that the EMG sensor must reach in order for any action to occur. Then, a new variable was initialized and made equal to the analog read of the EMG pin. This gives the output of the muscle movements read by the sensor. The code used various "if-then" statements, which state that if the value is higher than the threshold, then the movements of the fingers will occur. Six different movements were created from the program: all fingers open, all fingers close, two fingers open, two fingers close, one finger opens, and one finger closes. For the "all fingers" code, two servo motors were utilized because the servo motor was too small to be connected to the entire hand. The code below is for one finger opening/closing movements.

```
077-MyoWare-Muscle-Sensor
#include <Servo.h>

//Threshold for servo motor control with muscle sensor.
//You can set a threshold according to the maximum and minimum values of the muscle sensor.
#define THRESHOLD 200

//Pin number where the sensor is connected. (Analog 0)
#define EMG_PIN 0

//Pin number where the servo motor is connected. (Digital PWM 3)
#define SERVO_PIN 3


//Define Servo motor
Servo SERVO_1;

/*-------------------------------- void setup ----------------------------------------------*/

void setup(){

  //BAUDRATE set to 9600, remember it to set monitor serial properly.
  Serial.begin(9600);

  //Set servo motor to digital pin
  SERVO_1.attach(SERVO_PIN);


  SERVO_1.write(0);

/*--------------------------------  void loop  ----------------------------------------------*/
}
void loop(){

  //The "Value" variable reads the value from the analog pin to which the sensor is connected.
  int value = analogRead(EMG_PIN);



  //If the sensor value is GREATER than the THRESHOLD, the servo motor will turn to 180 degrees.
  if(value > THRESHOLD){
    SERVO_1.write(500);

  }

  //If the sensor is LESS than the THRESHOLD, the servo motor will turn to 0 degrees.
  else{
    SERVO_1.write(0);

  }



  //You can use serial monitor to set THRESHOLD properly, comparing the values shown when you open and close your hand.
  Serial.println(value);
}
```

Figure 1. One Finger Opening/Closing Mvmts Code

RESULTS

Total Participants	The location of the muscle sensor
23	Calf
13	Shoulder
7	Forehead
7	Back

Table 1. Location of Muscle Sensors on Participants

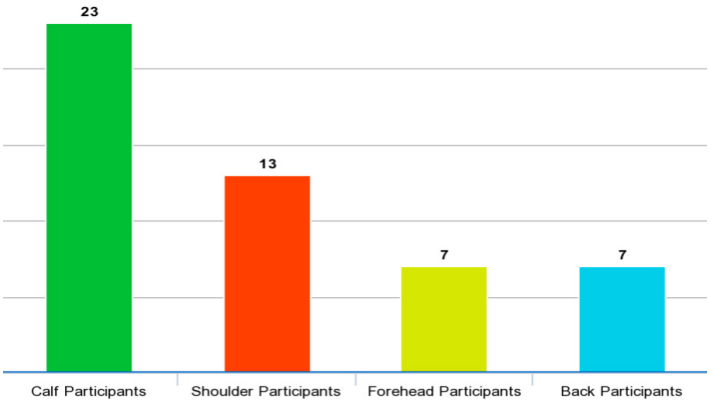

Figure 2. Location of Muscle Sensors Based off of Participants' Choices

The Different Combinations of Movements Programmed
5 fingers opened at same time
5 fingers closed at same time
2 fingers opened at same time
2 fingers closed at same time
1 finger opened at same time
1 finger closed at same time

Table 2. The Combinations of Movements Programmed

The data in Table 1 illustrates the results from a test of the muscle-controlled prosthetic by 50 participants. As seen above, the majority of people tested their arm when the sensor was on their calves. This shows that the prosthetic arm functions in the same manner as a human arm since the muscle sensor is placed on a different part of the body. The second most requested location was the shoulder. The least requested locations were the back and forehead. Six movements were created in total.

CONCLUSION

The overarching purpose of this experiment was to create an affordable prosthetic arm that could be controlled by muscle. The rationale for this project was to give people the option of prosthetics that require no mechanical changes to the body and are capable of completing the daily tasks required of a human arm.

The Johns Hopkins Applied Physics Lab conducted a study in which a prosthetic arm was controlled by brain waves (Gohd, 2018). This led to a prosthetic arm that would attach to the amputee and allow him to perform similar functions to his original arms. Instead of measuring the distance of the arm, which is what this research is about, the Johns Hopkins Lab measured the flexibility of the arm and the ability to make natural movements with a prosthetic arm. This correlates to this study because the movement of the fingers depends on the flexibility of the arm.

Another study was completed where a prosthetic arm was created with the power to be controlled by Bluetooth. An electrode ring called a myoband was attached to the arm like a bracelet, detecting the impulse in each muscle and sending the signals over Bluetooth to the miniature computer in the prosthetic hand. Then, the researchers were able to use the data on the computer to connect electrodes to the brain to analyze which parts of the brain were being stimulated when an amputee wanted to make a movement. This correlates with the research described in this paper because the distance applied from the prosthetic arm depends on the stimulation and transmission of our code, which directs movement to the arm (Whitwam, 2017).

One recommendation for the future is to test the prosthetic arm in more extreme situations and see its true capability. For example, heavy objects can be thrown on the arm to test durability, or the arm could be placed in extreme weather conditions such as heavy rain. Another recommendation for the future is to test which type of material is most effective for the functionality of the arm. As explained above, this arm would be tested in harsh conditions, so the most effective material for the arm could be tested in the process.

There were many limitations during the research project. For example, during the 3D printing stage, the arm had to be reprinted three times until a fully functioning hand was created properly. The position of the hand on CAD had to be changed

because the base of the hand was too fragile and could not support the rest of the hand. Another limitation was the difficulty of connecting all the parts together because the material would not stick to regular glue and required a more specifically designed adhesive.

REFERENCES

Amputee Statistics You Ought to Know. (n.d.). Retrieved from https://www.advancedamputees.com/amputee-statistics-you-ought-know

Carey, B. (2008, May 29). Monkeys Think, Moving Artificial Arm as Own. Retrieved October 25, 2018, from https://www.nytimes.com/2008/05/29/science/29brain.html

Gohd, C. (2018, February 3). Florida man becomes first person to live with advanced mind-controlled robotic arm. Retrieved from https://futurism.com/mind-controlled-robotic-arm-johnny-matheny

Massachusetts Institute of Technology. (2017, May 31). Making prosthetic limbs feel more natural: Muscle grafts could help amputees sense and control artificial limbs. *ScienceDaily*. Retrieved October 25, 2018 from http://www.sciencedaily.com/releases/2017/05/170531143621.htm

Mohney, G. (2013, April 24). Health Care Costs for Boston Marathon Amputees Add Up Over Time. Retrieved from https://abcnews.go.com/Health/health-care-costs-boston-marathon-amputees-add-time/story?id=19035114

Murphy, D. P., Bai, O., Gorgey, A. S., Fox, J., Lovegreen, W. T., Burkhardt, B. W., . . . Fei, D. (2017). Retrieved from https://www.ncbi.nlm.nih.gov/pmc/articles/PMC5736540/

Pitkin, M. R. (2014). Biomechanics of lower limb prosthetics. Place of publication not identified: Springer.

Whitwam, R. (2017, June 27). New Prosthetic Arm Powered by Bluetooth and Brainwaves - ExtremeTech. Retrieved from https://www.extremetech.com/extreme/248380-new-prosthetic-arm-powered-bluetooth-brainwaves

Woodford, C. (2010/2020) Prosthetic limbs. Retrieved July 16, 2020 from https://www.explainthatstuff.com/prosthetic-artificial-limbs.html

Enhancement of Chemotherapy Treatments Through Drug and Natural Product Combinations

Smrithi Balasubramanian[1], Sreevatsa Vemuri[1]
[1]duPont Manual High School
Louisville, Kentucky

ABSTRACT

To combat the issue of excessive, unwanted colon cancer cell growth, Fluorouracil, a common chemotherapy drug, is used. However, this drug can often have many negative side effects due to high toxicity levels, and cancer cells have also developed a form of resistance to the drug, causing even higher doses to be implemented. The purpose of this project was to use Urolithin, a beneficial microbial metabolite known to have drug-retaining abilities, and compare it against Withaferin (a plant-based derivative) in combination with Fluorouracil at varying doses in order to achieve a lower cell proliferation and growth rate at lower doses. Varying doses of Fluorouracil were used on the HT-29 colon cancer cell line, and a combination of varying doses of Fluorouracil and Urolithins at varying concentrations were tested on the same cell line and measured using an MTT assay for a comparative analysis. The same methodology was used for Withaferin. For the treatment of Fluorouracil alone, as the dose increased, the resulting cell proliferation and growth rates decreased. The combination treatment of Urolithins/Withaferin and Fluorouracil resulted in both lower cell proliferation and growth rates when compared to the treatment of Fluorouracil alone. This shows that lower Fluorouracil doses can be implemented in addition to Urolithin or Withaferin concentrations to achieve a lower proliferation and growth rate than standard treatment methods of the chemotherapy drug alone.

INTRODUCTION

There are various diseases in which abnormal cells rapidly divide uncontrollably and, in the process of doing so, destroy body tissue. The collective name for these diseases is known as cancer. Cancer is a genetic disease caused by changes to genes that control the way our cells function, including how they grow and divide ("What is Cancer," 2015). Normally, humans' cells go through the process of forming and dividing to form new cells as the body needs them. However, as cancer develops, this process breaks down, causing more damaged or abnormal cells to survive and extra cells to form. The formation of these extra cells plays a role in tumor growth. Cancerous tumors are malignant, meaning they can spread into nearby tissue and can travel to distant places in the body through the lymph system or blood ("What is Cancer," 2015). The spread of malignant tumors to surrounding tissue and nearby organs can cause serious and possibly fatal damage.

The third most common cancer in the world is Colon Cancer or Colorectal Cancer, and it is the second leading cause of cancer deaths ("What is Colorectal Cancer," 2018). Most colon cancer cases begin through the formation of a polyp, a cluster of cells on the lining of the colon or the rectum, but can later progress into more cancerous tumors.

The use of chemical substances or mixtures of chemical substances can be used to stop or slow the growth of the mentioned cancer cells. This process, also known as chemotherapy, works by targeting cells that grow or reproduce quickly, such as cancer cells. Chemotherapy is unlike more target-specific forms of treatment, such as radiation or surgery, because chemotherapy can affect the entirety of the body. The three main goals of chemotherapy are curing, controlling, and possibly palliating. Palliation is the intention to ease symptoms caused by cancer when it is at an advanced stage by improving the quality of life rather than completely curing it (American Cancer Society, 2018).

Oftentimes, however, chemo medication can affect healthy cells that also grow rapidly. Due to this characteristic, chemotherapy can often cause

detrimental side-effects. Common chemotherapy drugs include 5-Fluorouracil and Cisplatin. There are a number of healthy blood cells that can be affected by the therapy. White blood cells are a major candidate to be affected by the drugs, and as the white blood cell count lowers, the chance of receiving an infection rises. The medication can also reduce red blood cells and platelets, which can lead to anemia, fatigue, chest pain, bruising, bleeding, and more serious complications. In combination with blood cells, hair follicle cells can be affected, leading to hair loss. The cell lining in the stomach can be impacted, possibly leading to vomiting and diarrhea. Another common effect is hearing loss caused by high doses of chemotherapy, especially from drugs like Cisplatin (Cancer Net, 2018). These adverse side effects often last for long periods of time and can contribute to memory problems, weakening heart muscle, poor coordination, tired muscles, lower blood cell count, and an increase in inflammation (Nordqvist, 2017).

Along with these negative impacts of chemotherapy drugs, various cancer cell lines and tumors have developed a form of resistance to these drugs. In the past, the failure of these drugs has been linked to a protection system known as multi-drug resistance. Multi-drug resistance is caused by a protein membrane known as an adenosine-triphosphate binding cassette, which decreases the build-up of chemotherapy drugs in the cell by expelling them from the cancer cells, allowing the cancer tumors to form drug resistance (Liu, 2009). Additionally, drug resistance can be the result of another type of transport membrane protein known as solute carrier transporters because these proteins account for the chemo-sensitivity within the cells (Liu, 2009).

Microbiota, microorganisms found in multicellular organisms, play a vital role in cancer treatments. Commensal microbiota regulate physiological functions, including inflammation and immunity. This shows how microbiota play a beneficial role in the fight against cancer. A type of microbiota, microbial metabolites, regulate their own growth and development to encourage other organisms that are beneficial to them and suppress organisms that are harmful (BioAustralis, n.d.). They play an important role in the immune system by contributing to a barrier effect. Examples of metabolites include Urolithins, which are produced in the human gut and are found in the urine in the form of Urolithin B glucuronide after absorption of ellagitannins, as well as Ferrochrome, which is a cyclic hexapeptide.

Urolithins are intestinal microbial metabolites that are produced from foods containing ellagic acid and ellagitannin. A great example is pomegranates. In previous studies, both ellagitannins and ellagic acid have shown applicable biological impacts in humans that suggest potential preventive effects against chronic diseases such as cancer, diabetes, cardiovascular diseases, and neurodegenerative diseases (Espín et al., 2013). The study also noted that the health effects attributed to Urolithins based on studies carried out in vitro are numerous and distinct, and they can often include antimalarial properties and topoisomerase inhibition (Espín et al., 2013). Along with this, the gut microbiota also have a major role in defining the efficacy and toxicity of a broad range of drugs (Wilson & Nicholson, 2014). This study suggested that the microbial metabolites have a great drug-retaining ability, making them potential candidates to restrain the applied chemotherapeutic drugs within the cancer cells.

Taking this into context, this poses the overarching question: What is the effect of using Urolithins or Withaferin in combination with chemotherapy drugs such as 5-Fluorouracil and Cisplatin on colon cancer cells? The primary objective of this research is to reduce the dose of chemotherapy drugs by using beneficial substitutes while providing the same effective results of the chemotherapy treatment and decreasing the potential for detrimental side effects from the high toxicity levels of normal dose chemo drugs.

Previous studies have been conducted related to this research, but they have only included studying the effects of the microbial metabolites alone on cancer cell growth. The effects of lower amounts of chemotherapy drugs used in combination with microbial metabolites to improve treatment efficiency while still preventing the detrimental effects were not considered and are explored through this research.

This experiment tested the effects of ashwagandha (Withania somnifera), an all-natural herb from India, on colon cancer cell lines. Ashwagandha (more commonly known as Indian ginseng in English) is an ayurvedic herb, meaning that it is used in medicine with no added chemicals.

Ayurvedic medicine has been used for thousands of years and has been effective against many diseases. Ashwagandha has been known for its anti-cancerous properties and its ability to ease pain and swelling and reduce stress and anxiety (Spritzler, 2019).

Within cancer, ashwagandha has been effective mainly because it enhances immune cells and can damage the cancer cells' ability to regenerate ("Ashwagandha," 2018). Ashwagandha has been described as having "neuroprotective and anti-inflammatory properties" based on in vitro studies (Palliyaguru et al., 2016). In addition, ashwagandha creates an antioxidant that helps protect normal cells while also creating a pro-oxidant that fights the cancer cells and stimulates certain proteins that help keep regular cells stable (Berg et al., n.d.). Lastly, it stops angiogenesis, which is the creation of blood vessels (lymph nodes) that contribute to the growth and spread of cancer cells (Berg et al., n.d.).

In contrast to the research done by MSKCC, the National Cancer Institute, and NCBI, this experimentation determined a way to mitigate the effects of colon cancer using combination treatments, rather than testing ashwagandha on other types of cancer and analyzing how different chemical agents of ashwagandha can be used in mitigating colon cancer effects. For example, in the research done by Palliyaguru in NCBI, the group tested ashwagandha's "withanolide Withaferin A" on cancer. This experimentation works with the ashwagandha extract from the roots of the herb, which is all-natural. The in vivo studies done by MSKCC tested the effects of other supplements rather than ashwagandha on cancer. This experimentation focused on mitigating the effects of colon cancer in the early stages rather than later stages.

Using the information presented by the research groups, it can be concluded that the anti-cancer properties that ashwagandha portrays and the stage-based development of colon cancer allow ashwagandha to decrease and slow the growth of colon cancer cells, thus mitigating the effects of cancer. Therefore, it can help resolve the overall problem of finding an all-natural way of reducing cancer effects.

Due to the known beneficial properties of both additives, it can be hypothesized that the use of Urolithin or Withaferin-A in combination with chemotherapy drugs of a lower dosage will reduce the harmful effects and toxicity of chemotherapy and produce the same beneficial outcome of eliminating cell growth. In addition, the preliminary hypothesis for the testing of two natural products (ashwagandha and pomegranate juice) was that the highest concentration of a natural product that is not in combination with a chemotherapy drug would provide a decrease in cancer cell growth and viability, serving as a more accessible, feasible, and easier alternative when dealing with colon cancer.

METHODOLOGY

For this experimentation, a series of three major steps were taken to complete the trials. The first step was preparing the cells in the well plate. A T25 flask that held the cell line was obtained. The old medium that was in the flask was first aspirated to later be replaced with new medium. In order to do this process efficiently, the flask was tilted to prevent the aspiration of the cells. A phosphate buffer solution (PBS) was used to clean out the flask completely by shaking the flask up and down. This is necessary because when the enzyme trypsin is used to separate the cells from the flask, there cannot be any medium, or else it will inactivate the trypsin's function. 5 mL of PBS was used to clean out the flask and was added through a 10 mL pipette. The PBS was then aspirated. This process was done twice to ensure that the medium was fully removed. 1.5 mL of trypsin was then added using the electronic pipette controller and a 5 mL tip, and the flask was gently shaken to allow the trypsin to cover more area. This was done quickly, and the flask was then put into the incubator for five minutes.

After the flask was removed from the incubator, the trypsin-cell mixture was pipetted out of the flask and into a new 15 mL tube. 5 mL of new medium was added to the mixture, and it was resuspended using a 10 mL pipette. The trypsin-cell-medium mixture was then taken to a centrifuge, and a balance with an equal volume to that of the mixture was placed on the opposite side of the centrifuge. The mixture and the balance were both placed into the centrifuge for 5 minutes at 1500 revolutions per minute (RPM). After 5 minutes, the two tubes were taken out of the centrifuge. A cell pellet formed at the bottom of the tube, and the medium and trypsin solution formed at the top. The

trypsin and medium were then aspirated carefully out of the tube, leaving only the cell pellet at the bottom. 10 mL of new medium was added to the cell pellet tube, and the cell pellet was then resuspended in the new medium.

10 mL of new medium was used since the recommended volume for new medium in a T25 flask is ten mL. 1 mL of the cell-medium mixture was taken and was counted using a hemocytometer. This process helped to determine the number of cells and amount of new medium that were needed to get 10,000 cells in each well plate. This number varied for each trial. In a petri dish, 9 mL of the new medium and 1 mL of the cell solution was added (these numbers were about the same for each trial). The petri dish was thoroughly mixed to allow the cells to spread. A 96 well plate was then taken and using a multichannel pipette, 100 uL of the petri dish mixture was added to each well along with 100 uL of new medium. Finally, the well plate was taken to the incubator, where the cells grew at 36° Celsius with 5% CO2.

The second step of the experimentation was to add the compound to the cells. After waiting 24 hours for the cells to grow, the compound/extract was added. When adding the extract (Withaferin-A and Uro-A), a serial dilution was done to allow for different concentrations or dosages. Four different treatments were used against the cells. One included Withaferin-A in concentrations of 10 uM, 5 uM, 2.5 uM, 1.25 uM, and 0.625 uM. The second treatment was Withaferin-A at 10 uM (constant) with varying doses of 5-Fluorouracil, starting at 10 uM and going to 0.625 uM. 5-Fluorouracil works against cancer cells but only at high concentrations because the cells have built up a resistance against the drug. The main purpose of using 5-Fluorouracil was to see if the extract could work with the 5-Fluorouracil at low dosages to inhibit the growth of cells. The third treatment was Uro-A at a constant of 100 uM along with varying dosages of 5-Fluorouracil, starting at 10 uM and ending at 0.625 uM. The last treatment was only 5-Fluorouracil at varying dosages, starting at 10 uM and ending at 0.625 uM. Uro-A was not tested by itself because it has already been heavily researched and is known to be most effective at 100 uM.

A stock solution was prepared for each treatment in a microcentrifuge tube. 1250 uL, or 1.25 mL, of medium was added to the four stock solution tubes using a handheld pipette with a 100 uL tip. A 1250/50 dilution was done, and each of the compounds was added to the stock solution. Using a microcentrifuge rack, five different microcentrifuge tubes were placed in order and labeled 1-5. Each tube was also given 300 uL of DMSO and medium mixture to help the compound dissolve. 300 uL was taken from the stock solution and added to the first tube, and the first tube was then vortexed using the vortex mixer. After the tube was vortexed, 300 uL was taken and then added to the second tube. This process was done five times for all five tubes, which allowed for different concentrations. The 96-well plate was then taken from the incubator, the old medium was removed using the multichannel pipette, and 100 uL of new medium was added. An MTT Assay was then performed in order to assess the cells' metabolic activity. From the assay, cell proliferation rates were collected using a spectrophotometer in order to analyze changes in cell growth and cell proliferation rates.

RESULTS

A two-sampled statistical t-test was performed, and it compared the percent of cells remaining within the Fluorouracil treatment to the combination treatments of Uro-A 50uM (plus varying concentrations of Fluorouracil), Uro-A 100uM (plus varying concentrations of Fluorouracil), and 2.5uM of Withaferin-A (plus varying concentrations of Fluorouracil). The t-test compared the treatments at one specific concentration, meaning that the t-test value for 5uM of only Fluorouracil was compared with the 5uM value in one of the treatments. The degrees of freedom used for each test was two, which is derived from subtracting the number of trials by one. In this case, a total of three trials were conducted for each treatment at each concentration, resulting in two degrees of freedom. Lastly, the p-value at 0.05 significance with 2 degrees of freedom is 4.303, which is used to compare the test score. If the test value is less than 4.303, this means the data is not as significant, and if it is greater than 4.303, the data is significant in showing the percent decrease or percent of cells remaining.

t-Test (50uM UroA + 5FU)		
	50uM UroA	p-value
0.3125uM	1.52157169	<4.303
0.625uM	2.90986245	<4.303
1.25uM	3.69563377	<4.303
2.5uM	3.9554963	<4.303
5uM	6.60012906	>4.303

Table 1: T-Test for 50uM Uro-A Plus Varying Concentrations of FU

t-Test (100uM UroA + 5FU)		
	100uM UroA	p-value
0.3125uM	1.90883559	<4.303
0.625uM	4.31148153	>4.303
1.25uM	4.76940688	>4.303
2.5uM	3.15320935	<4.303
5uM	6.87904477	>4.303

Table 2: T-Test for 100uM Uro-A Plus Varying Concentrations of FU

t-Test (2.5uM WA + 5FU)		
	2.5uM WA	p-value
0.3125uM	7.41865623	>4.303
0.625uM	10.6835763	>4.303
1.25uM	9.79505482	>4.303
2.5uM	5.87447268	>4.303
5uM	9.13041877	>4.303

Table 3: T-Test for 2.5uM Withaferin-A Plus Varying Concentrations of FU

Tables 1-3 compare 50uM UroA, 100uM UroA, and 2.5uM Withaferin-A in combination with the Fluorouracil as one sample, with the other sample being the treatment with only Fluorouracil. The general trend for these t-tests was that as the concentration increased from 0.3125uM to 5uM, the t-test value increased, showing that the data became more significant in reducing the cells. This proves that the data is statistically important and corresponds with the overall decrease in the raw data of the reduction of cell viability.

Concentration	Mean	Standard Deviation	Number of trials
0.3125uM	105.536669	17.5162	3
0.625uM	106.097705	12.6292	3
1.25uM	91.7558564	11.3389	3
2.5uM	91.3596233	19.3839	3
5uM	92.0934668	12.8638	3

Table 4: Descriptive Stats for Fluorouracil Treatment Only

Concentration	Mean	Standard Deviation	Number of trials
0.3125uM	89.995107	2.4838	3
0.625uM	84.4054282	2.6874	3
1.25uM	66.9578626	2.5501	3
2.5uM	45.986688	4.3595	3
5uM	40.9305501	3.8464	3

Table 5: Descriptive Stats for Uro-A 50uM Plus Varying Concentrations of Fluorouracil

Concentration	Mean	Standard Deviation	Number of trials
0.3125uM	86.1503431	1.6192	3
0.625uM	73.6821663	3.1753	3
1.25uM	59.7421532	2.5676	3
2.5uM	50.1993214	11.638	3
5uM	38.6361284	3.9611	3

Table 6: Descriptive Stats for Uro-A 100uM Plus Varying Concentrations of Fluorouracil

Concentration	Mean	Standard Deviation	Number of trials
0.3125uM	30.3462521	1.1647	3
0.625uM	28.0369963	0.8137	3
1.25uM	27.1497762	1.3930	3
2.5uM	25.528878	1.0013	3
5uM	24.1992684	0.6385	3

Table 7: Descriptive Stats for Withaferin-A 2.5uM Plus Varying Concentrations of Fluorouracil

The descriptive stats shown in tables 4-7 observe the mean, standard deviation, and the number of trials conducted at each concentration level. The mean shows the average percent of cells remaining out of 3 trials, and the standard deviation is taken from the 3 trials done for each

concentration. A trend can be analyzed from the figures: as the concentration increased, the cell viability decreased. It can also be concluded that 2.5uM of Withaferin-A, in combination with the Fluorouracil, provided the best results in having low cell viability.

In addition, the averages were graphed to show the trend line and dose curve for the cell viability for each of the treatments. The graphs are listed below with their respective error bars.

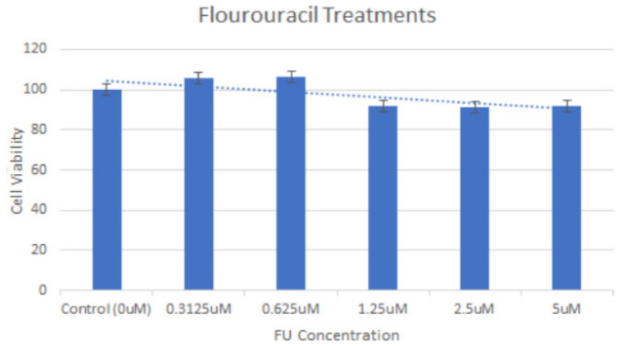

Figure 1: Mean of Fluorouracil Treatments vs. Cell Viability

Figure 1 illustrates what standard chemotherapy treatments for colon cancer using Fluorouracil would yield. As the concentration of the drug increased, the overall cell viability was not majorly impacted, but there was a slight decrease. Figure 2 shows the combination treatments of both Urolithin concentrations at 50 uM and 100 uM in comparison to only Fluorouracil treatment. As the concentration of Fluorouracil increased in combination with either Urolithin concentration, resulting cell viability decreased. However, as the concentration of Urolithin increased from 50 to 100 uM, the resulting cell viability was lower at all levels of Fluorouracil concentrations.

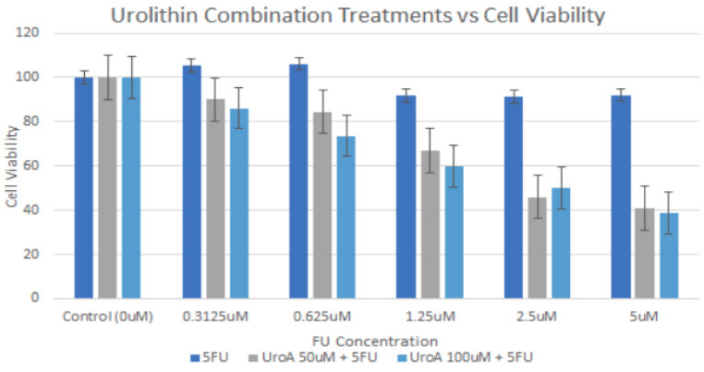

Figure 2: Mean of 50 and 100 uM Urolithin Combination Treatments vs. Cell Viability

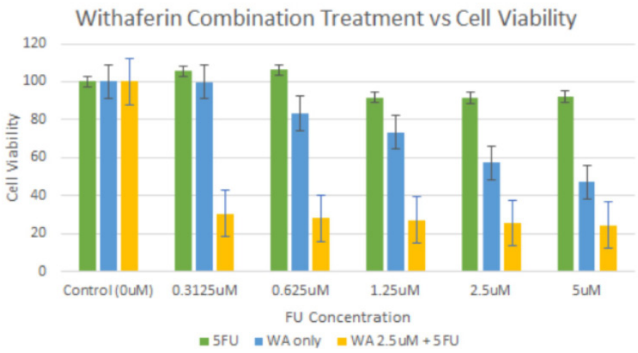

Figure 3: Mean of Withaferin-A Combination Treatment vs. Cell Viability

The graph above shows a comparison of three treatments, including only Fluorouracil, only Withaferin, and Withaferin at 2.5 uM in combination with Fluorouracil. For treatments including Fluorouracil, as the concentration of Fluorouracil increased, the resulting cell viability decreased. For the Withaferin only treatment, as the concentration of Withaferin increased, the resulting cell viability decreased and was lower than that of the Fluorouracil-only treatment at all concentrations. However, the lowest cell viability at all levels was achieved by the combination treatment of Withaferin at 2.5 uM and Fluorouracil.

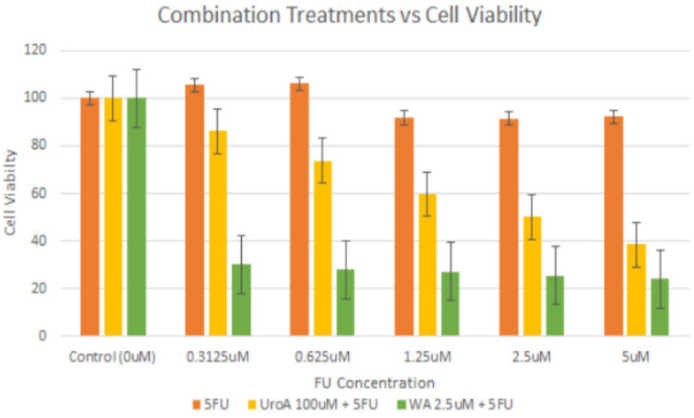

Figure 4: Comparison of the Mean of All Combination Treatments vs. Cell Viability

The graph above compares the best treatment for the desired purpose of the Urolithin portion and the Withaferin portion and compares this to the Fluorouracil-only treatment. It shows that the Urolithin treatment at 100 uM in combination with Fluorouracil had lower cell viability at all levels than the Fluorouracil-only treatment. The treatment of Withaferin at 2.5 uM in combination with Fluorouracil produced the lowest cell viability

at all levels of Fluorouracil concentration compared to all treatments tested.

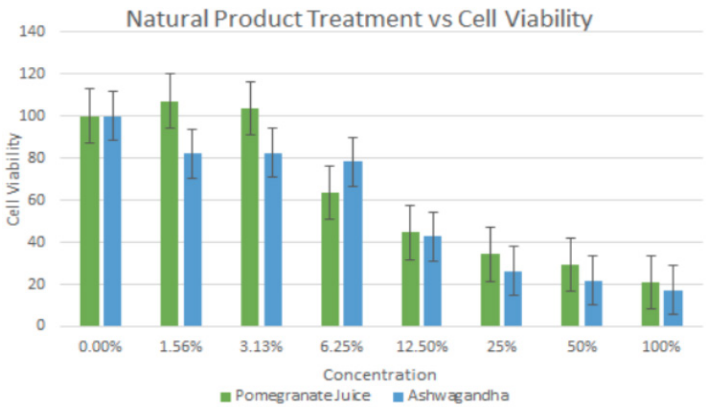

Figure 5: Preliminary Trial - Ashwagandha and Pomegranate Juice vs. Cell Viability

Figure 5 examines the effects of natural products vs. cell viability. The natural products used were ashwagandha, which Withaferin-A is derived from, and pomegranate juice, which Uro-A is derived from. Both showed very significant levels of cell decrease, with ashwagandha decreasing the cell viability by 83% and pomegranate juice decreasing the cell viability by about 80%. This goes to show how natural products are very efficient in reducing cell viability without the presence of a chemotherapy drug. This is important since natural products are more feasible and available to use compared to chemicals.

DISCUSSION & CONCLUSION

Chemical substances are used to stop or slow the growth of cancer cells. This process, also referred to as chemotherapy, works by targeting cells that grow or reproduce quickly, just as cancer cells do. Chemotherapy is unlike other forms of more targeted reduction like radiation or surgery because it can affect the entirety of the body. However, chemo medication can often affect healthy cells that also grow rapidly. Due to this characteristic of chemo medication, chemotherapy can often cause detrimental side-effects. Along with these negative impacts of chemotherapy drugs, various cancer cell lines and tumors have developed a form of resistance to these drugs. This experiment's main goal was to reduce the dose of the chemotherapy drugs by using beneficial microbial metabolites and plant-based products while providing the same effective results of the chemotherapy treatment without the detrimental side effects stemming from high toxicity levels of normal dose chemo drugs.

The overall results suggest that in the experimentation of three trials of Withaferin-A, there was an 80% decrease in the levels of cell viability. According to an in vitro and in vivo study done by Sham S. Kakar and his colleagues, Withaferin-A inhibits tumor growth and prevents metastasis from occurring within cancer cells. In addition, it targets spheroid formation in ovarian tumors when in combination with Cisplatin, which is another chemotherapy drug (2012). Last but not least, the cause for cell death is explained by Yue Yu, with Withaferin-A having antitoxic and antitumor properties (2017). The 50 uM Urolithin combination with Fluorouracil showed a cell decrease by 60% within 24 hours, while the 100 uM Urolithin combination with Fluorouracil showed a cell decrease of a little greater than 60%. This makes sense because a higher concentration of Urolithin showed signs of greater cell decrease compared to a lower dose of Urolithin. However, Withaferin-A was tested at 2.5 uM. This could be because Withaferin-A is much more effective at lower concentrations.

Major findings that were gathered included that when Withaferin-A was in combination with the Fluorouracil drug, it proved to be the most effective in reducing cell viability and growth. The data showed consistent levels of cell decrease of around 80% within 24 hours, and this compares to the Urolithin combination since those treatments had a cell decrease of around 60% at the highest concentration of Fluorouracil. In addition, the ashwagandha at a 100% concentration reduced the cell growth by 83% in 24 hours, while the pomegranate juice decreased the cell growth by 79%, showing how these everyday natural products go one step further in serving as accessible and feasible ways of reducing the harms of colon cancer without the need of chemotherapy treatments.

Previous studies related to this research have been conducted, although they have only included the effects of the microbial metabolites alone on cancer cell growth, while others used the extracts in combinations with chemotherapy drugs. The effects of low quantities of chemotherapy drugs used in combination with microbial metabolites to improve treatment efficiency while still preventing detrimental effects were not considered. Both of

the derived extracts in this project have not been extensively tested yet, meaning that the research can be minimally compared to previous studies. When compared to other treatments on cancer cells, the combination treatments tested in this experiment provide for lower cell viability. Microbial metabolites could be tested on other cancer cell lines to see if they produce the same effect and if they can be utilized in the treatment of other cancers.

To improve the experimental design for future procedures, a cell incubation period with the addition of the compound for 48 hours could provide more evident trends and clearer results than an incubation period of 24 hours. Experimental error is indicated through the inaccurate serial dilution of the natural products and sterilization of the laboratory hood. These errors were most likely caused by a time strain and the need to put the cells back into the incubator; however, these trials were repeated, and measures were taken to try and avoid such mistakes. None of the analyzed results were affected by uncontrolled events because the experiment was conducted in a controlled environment. In addition, other microbial metabolites, such as Ferrichrome, could be utilized in combination with Urolithins, alone, or with Fluorouracil. Other common chemotherapy medications, such as Cisplatin, could be tested in the same experimental design and utilized on the cancer cell lines most commonly treated with the drug.

ACKNOWLEDGEMENTS

We would like to thank our mentors, Dr. Venkatakrishna Jala and Dr. Shoba Bodduluri, for providing us with the necessary equipment and testing environment, as well as for guiding us through this research and its corresponding analysis.

REFERENCES

American Cancer Society. (2018). How Is Chemotherapy Used to Treat Cancer? Retrieved from https://www.cancer.org/treatment/treatments-and-side-effects/treatment-types/chemotherapy/how-is-chemotherapy-used-to-treat-cancer.html

Ashwagandha. (2018, April 13). Retrieved October 26, 2018, from https://www.mskcc.org/cancer-care/integrative-medicine/herbs/ashwagandha

Berg J, Weinstein MJ, Schelling SH, Rand WM. Treatment of dogs with osteosarcoma by administration of cisplatin after amputation or limb-sparing surgery: 22 cases (1987-1990). *J Am Vet Med Assoc*. 1992;200(12):2005-2008

BioAustralis. (n.d.). What are metabolites? Retrieved from http://www.bioaustralis.com/metabolites.htm

Cancer Net. (2018, October). Hearing Problems. Retrieved from https://www.cancer.net/coping-with-cancer/physical-emotional-and-social-effects-cancer/managing-physical-side-effects/hearing-problems

Espín, J. C., Larrosa, M., García-Conesa, M. T., & Tomás-Barberán, F. (2013). Biological Significance of Urolithins, the Gut Microbial Ellagic Acid-Derived Metabolites: The Evidence So Far. *Evidence-Based Complementary and Alternative Medicine*, 2013, 1-15. doi:10.1155/2013/270418

Kakar, S. S., Jala, V. R., & Fong, M. Y. (2012). Synergistic cytotoxic action of cisplatin and withaferin A on ovarian cancer cell lines. *Biochemical and biophysical research communications*, 423(4), 819–825. https://doi.org/10.1016/j.bbrc.2012.06.047

Liu, F. (2009). Mechanisms of Chemotherapeutic Drug Resistance in Cancer Therapy—A Quick Review. *Taiwanese Journal of Obstetrics and Gynecology,* 48(3), 239-244. doi:10.1016/s1028-4559(09)60296-5

Nordqvist, C. (2017, December 14). Chemotherapy: What it is, what to expect, side effects, and outlook. Retrieved October 01, 2018 from https://www.medicalnewstoday.com/articles/158401.php

Palliyaguru, D. L., Singh, S. V., & Kensler, T. W. (2016, January 29). Withania somnifera: From prevention to treatment of cancer. Retrieved from https://www.ncbi.nlm.nih.gov/pmc/articles/PMC4899165/

Spritzler, F. (2019). 12 Proven Health Benefits of Ashwagandha. Retrieved July 16, 2020, from https://www.healthline.com/nutrition/12-proven-ashwagandha-benefits

What Is Cancer? (2015). Retrieved from https://www.cancer.gov/about-cancer/understanding/what-is-cancer

What is colorectal cancer, colon cancer and rectal cancer? (2018). Retrieved from https://www.ccalliance.org/colorectal-cancer-information/what-is-colorectal-cancer

Wilson, I. D., & Nicholson, J. K. (2014). The Modulation of Drug Efficacy and Toxicity by the Gut Microbiome. In S. Kochhar & F. Martin (Authors), *Metabonomics and gut microbiota in nutrition and disease* (pp. 323-341).

Yu Y, Katiyar SP, Sundar D, et al. Withaferin-A kills cancer cells with and without telomerase: chemical, computational and experimental evidences. *Cell Death Dis*. 2017;8(4):e2755. Published 2017 Apr 20. doi:10.1038/cddis.2017.33

Development of a Novel Water Filter to Remove Pharmaceuticals from Water Using Various Carbon-Based Nanomaterials

Jane Hu[1], Ellie Hummel[1]
[1]duPont Manual High School
Louisville, Kentucky

Project Advisors: Dr. Ming Yu, University of Louisville. Dr. Manasa Sunkara, University of Louisville. Ms. Kathy Fries, duPont Manual High School.

ABSTRACT

The purpose of this project was to develop an effective method to remove pharmaceuticals. To combat the ineffectiveness of some current treatments, this project analyzed and compared the interactions between pharmaceuticals and various carbon-based nanomaterials. This research specifically targeted the removal of estradiol, a common form of estrogen, by graphene and carbon nanotubes. The nanomaterials' effectiveness was measured by using the absorbency energies between estradiol and each nanomaterial and by observing the pre and post-interaction structures of the graphene and carbon nanotubes. This data was collected from a state-of-the-art computational simulation model based on first principle calculations, Density Functional Theorem. Graphene was found to have significantly higher absorbency energies than carbon nanotubes, and the graphene structures were undamaged by estradiol, indicating that graphene attracts pharmaceuticals and can be reused. In the future, graphene will be used to develop a water purification device.

Key Words: Carbon nanotubes, graphene, water purification, DFT, estradiol, pharmaceuticals, drugs, nanomaterials
Abbreviations and Acronyms: Density Functional Theorem (DFT)

INTRODUCTION

Pharmaceuticals In Drinking Water

Over the past decade, pharmaceutical remains in the water supply have garnered worldwide attention. Currently, an estimated 41 million people in the U.S. are exposed to drug contaminated water every day [5]. In fact, in a study conducted by the U. S. Geological Association, traceable amounts of pharmaceuticals were found in over 80 percent of water samples taken from various streams and water supplies [15]. Among these were over fifty-one different pharma compounds, such as antidepressants, blood thinners, heart medications, hormones, and painkillers [15] [8]. Unfortunately, these numbers are only growing due to a combination of poor waste disposal methods, accidental spills, and sparse regulations [30].

While the scope of the impact of these contaminants remains unknown, many health problems have been associated with trace amounts of pharmaceuticals. Nasser Nassiri Koopaei and Mohammad Abdollahi of the Department of Toxicology at Tehran University found that "their unknown toxicity, teratogenicity[1] and carcinogenicity[2] profile associated with lack of monitoring and control measures impose a significant hazard risk on the public health" [6]. More specifically, pharmaceuticals may significantly affect receptor proteins in the brain by disturbing hormonal and genetic receptor proteins [11] [7]. Furthermore, other side effects are possible, such as the evolution of antibiotic-resistant pathogens. Already, antibiotic-resistant genes have been found in biofilms inoculated with drinking water bacteria in Germany. A study conducted at the University of Hong Kong found that certain known

1 An agent that can disturb the development of the embryo or fetus, often resulting in birth defects
2 Substance that promotes the formation of cancer
3 Common methods include biological oxidation/biodegradation, activated carbon adsorption, ozonation, electrodialysis, reverse osmosis, sedimentation, filtration and coagulation/flocculation.

pharmaceutical contaminants could lead to increased allergies, particularly in youth [21]. Thus, the potential health implications of life-long exposure to trace levels of pollutants are severe and, more importantly, remain a largely unexplored area of toxicology.

Despite these health threats, conventional methods of water purification fail to remove emerging contaminants [20]. The most common method for water purification, reverse osmosis, was found to only remove forty-five percent of pharmaceuticals [32][33]. According to the World Health Organization, some conventional methods remove as little as 5% of pharmaceuticals, much lower than acceptable ranges [41][12]. Additionally, these methods are uneven in their approach. Research has shown that while some conventional treatment methods have resulted in a ninety percent removal rate in some pharmaceuticals like ibuprofen and naproxen, they have little to no effect on other pharmaceuticals like carbamazepine [15]. Therefore, conventional methods lack two main aspects. Primarily, they leave large amounts of pharmaceuticals in the water supply during the purification process. Moreover, pharmaceuticals clog the filters, and due to the nature of the bonds, the filters can not be cleaned and reused, resulting in frequent replacement. These replacements increase the cost, making adequate water purification inaccessible [35].

Use of Nanomaterials for Water Purification

There has been a growing interest in using nanomaterials for water filtration. Nanomaterials have a greater relative surface area in relation to other materials used in water purification, enabling them to remove smaller contaminants. Furthermore, nanomaterials are less costly to maintain. For instance, conventional methods struggle to prevent the growth of microorganisms that degrade the filters, requiring frequent replacement of the filters. However, certain types of nanomaterials are able to prevent microorganisms from developing on the materials, thereby decreasing costs and increasing effectiveness [24].

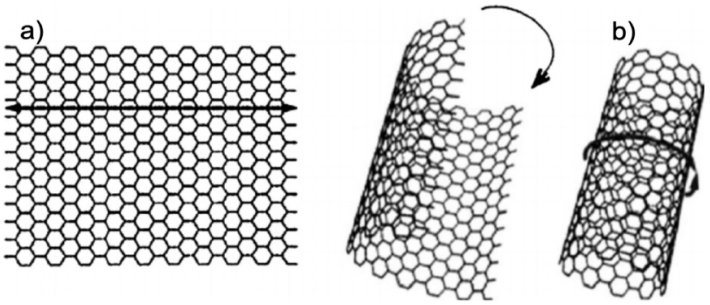

Figure 1. Graphene (Left) vs. Carbon Nanotubes (Right) [42]

In particular, two types of nanomaterials were of interest: graphene and carbon nanotubes. Graphene is made up of covalently bonded carbon atoms, which form a sheet of continuous hexagonal tiling. Similarly, carbon nanotubes are made of covalently bonded carbons that form a hexagonal pattern. However, instead of forming a flat sheet, the sheet is rolled up to make a cylindrical shape. These tubes are usually 0.1 - 0.4 nanometers in diameter and several microns in length [6].

Carbon nanotubes and graphene have many potential environmental remediation and wastewater applications [16][17][27][25]. Carbon nanotubes have incredibly high van der Waals indexes, allowing them to attract large polar covalent molecules such as pharmaceuticals [17] [26]. Furthermore, their mechanical and chemical properties have "exceptional water and wastewater treatment capabilities and have proved to work effectively against both chemical and biological contaminants" [31].

Many additional properties of carbon nanotubes and graphene make them advantageous over other nanomaterials. According to a study done by Muhammad Tahir Amin, the Alamoudi Water Research Chair at King Saud University, carbon nanotubes absorb more organic compounds from water due to their "high specific surface area, assessable adsorption sites...tunable surface chemistry, and reusability" [3]. Both of these materials have also shown great promise in removing heavy metals and organic matter from water [10][37]. Moreover, carbon nanotubes and graphene can now be mass-produced due to advancements in research [9]. All of these properties allow carbon-based nanomaterials to be less costly and have a greater attraction towards aqueous molecules.

Literature Review of Relevant Sources

Little research has been conducted to explore the use of nanomaterials for the targeted removal of pharmaceutical drugs. Current research focuses on nanofiltration, a process that employs the previously mentioned nano-membranes. The use of nano-adsorbents, the group of nanomaterials containing carbon and graphene, has been largely dismissed [4]. In a study done by Yonggang Wang et al. of the School of Environmental Science and Engineering at Tianjin University of China, nanofiltration was combined with reverse osmosis to create a system that removes pharmaceuticals at a greater rate than conventional methods. The results showed that when they combined the two techniques, over ninety-five percent of pharmaceuticals were removed compared to the forty-five percent and fifty percent using reverse osmosis and nanofiltration alone, respectively [32][33]. Furthermore, a study by Gordon Yang and Chia-Heng Yen, who are associated with the Institute of Environmental Engineering at the National Sun Yat-Sen University of Taiwan, had a different technique in applying nanofiltration to remove pharmaceuticals; instead of combining nanofiltration with conventional water purification methods, the researchers analyzed different interlayer materials used in conjunction with the filtration system. The results showed that various materials could remove a majority of certain pharmaceuticals but have removal rates of less than seventy-five for other pharmaceuticals [38]. Both of these studies came to the same conclusion—nanofiltration could be used to make a water filter that removes pharmaceuticals at acceptable rates. However, nanofiltration is both expensive and hard to mass-produce, while nano-absorption could be more feasible and allow for increased access. Overall, sparse research has been done using carbon-based nanomaterials such as carbon nanotubes and graphene for the targeted removal of pharmaceuticals.

Project Objectives

Due to the prevalence of pharmaceuticals in the water supply and lack of research in the field, a more accessible water filter must be developed to remove pharmaceuticals at acceptable rates. Specifically, the interactions between nanomaterials and the drug estradiol were examined. Estradiol is a popular form of estrogen, a female sex hormone produced by the ovaries. It is used to treat menopause symptoms such as hot flashes, and vaginal dryness, burning, and irritation [34]. Estradiol poses an extreme health risk to those who may consume it, even in small amounts in the water supply. In fact, these types of hormonal pharmaceuticals "have high bioaccumulation potential, which can have adverse effects on hormonal control" [20]. Furthermore, estradiol has the same hexagonal shape as most steroids, a group of pharmaceuticals that make up a majority of pharmaceutical contaminants. Therefore, a filter designed using estradiol could be applied to steroids and other similar drug types. The functional group hydroxide, located on each end of estradiol, is also common among pharmaceuticals. Thus, due to its popularity, potential health effects, and applicability to other pharmaceuticals, estradiol was explored in this study.

The purpose of this project was two-fold. The researchers explored estradiol's interactions between carbon nanotubes and graphene to determine whether the nanomaterial could remove estradiol from water. Then, the carbon nanotubes and graphene interactions were compared to determine which nanomaterial was more effective at removing estradiol from water. There is currently no research on possible methods for targeting the specific removal of the pharmaceutical drug estradiol. Furthermore, no studies have compared the effectiveness among various carbon-based nanomaterials to determine which of them is the most effective at removing pharmaceutical drugs from water.

This research will provide a theoretical understanding of the interactions between pharmaceuticals and carbon-based nanomaterials. Using this framework, future engineers will be able to test these nanomaterials in a lab setting and potentially develop a water filter that removes pharmaceuticals. Additionally, because nanomaterials are now easy to mass-produce, these water filters could be drastically cheaper than conventional filters and increase access to affordable, clean water.

METHODOLOGY

1. Computational Details

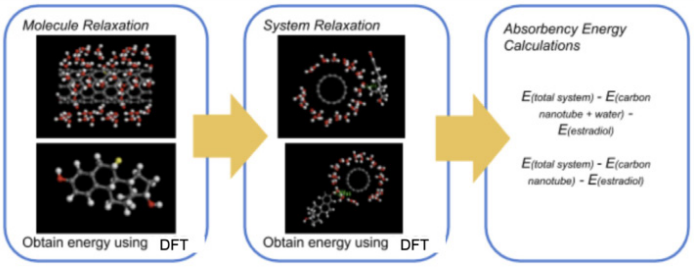

Figure 2. Method Overview. The absorbency energies resulted from the third step of the process, while the pre and post-interaction structures of the carbon nanotubes and graphene were determined from the beginning and end of the second process.

The research used a quantitative and qualitative quasi-experimental research design using computational simulations. This project analyzed two aspects of the interactions between the nanomaterials and the pharmaceutical. First, the absorbency measures were analyzed. These absorbency energies are a measure of the attraction between estradiol and the nanomaterial. The absorbency energies allowed the researcher to determine 1) whether the attraction was strong enough between the pharmaceutical and nanomaterial for the nanomaterial to remove estradiol from the aqueous solution and 2) if so, whether carbon nanotubes or graphene had a greater efficiency at removing estradiol from water. Absorbency energies between -0.4 and -0.8 electron volts indicated a strong physical absorption and, therefore, that the nanomaterial could remove the pharmaceutical. Second, the structures before the interaction with the pharmaceutical, or the pre-relaxation structures, were compared with the structures after the pharmaceutical had interacted with the nanomaterial, the post-relaxation structures. Comparing these structures allowed the researcher to determine whether there was any damage done to the nanomaterial and whether the nanomaterial could be reused.

This process had three main steps. First, the individual molecules of the carbon nanotube; graphene; graphene and water; carbon nanotube and water; and estradiol were relaxed, or the ground state was found, and the total energy of the molecules was recorded. Then, using these relaxed structures, systems were created that contained the nanomaterial and pharmaceutical. These were once again relaxed, and the energy was recorded. Finally, the absorbency was calculated and analyzed using the recorded energies, and the pre and post-relaxation structures were compared.

The Density Functional Theorem framework was employed to perform the structure relaxation. DFT is a state-of-the-art computational simulation model that uses quantum mechanical equations based on first principle calculations to situate the atoms in the ground state. Once in this relaxed position, DFT calculates the total energy of the system used in the later absorbency energy calculations and outputs the structures for comparison. DFT has been perfected by many scientists. Furthermore, the equations used by DFT have been vigorously proven, so the calculated ground states are highly accurate [18][14]. DFT is also used by many prominent scientists in the fields of chemistry, material science, and physics to study the theoretical properties of molecules at the atomic level [28][40].

2. Obtaining Energy of the Individual Structures

Four input files were created and modeled after codes and guidelines provided in the DFT user manual [19]. These files were made in a LINUX machine. This machine used Fortran to code and was chosen due to its large storage space. The first of these files was called POSITION. POSITION described the structure of the molecules and the Brillouin zone that contained the molecules. The first three lines contained three vectors in the form <x,0,0>, <0,y,0>, and <0,0,z>, which describe the dimensions of the Brillouin zone that contains the structure described by the coordinates later in the code. DFT uses a periodic system, meaning that this zone and the structure inside the zone gets repeated in every direction to form a repeating figure that spans 3D space. Therefore, it was important to 1) ensure that the structure described in the remaining part of the program did not exceed the zone to prevent any overlap and 2) ensure that the zone was large enough to prevent any interactions between zones. A Brillouin zone of <17.14,0,0>, <0,20,0>, and <0,0,20> was carefully checked by examining the change of the total energy of the molecules with

increasing Brillouin zones.

The next line contained three numbers that described the number of carbon atoms, hydrogen atoms, and oxygen atoms. After creating the next section of the file, these numbers were found by counting. After this line, the coordinate system was declared as a cartesian coordinate system. The rest of the file contained four columns. These four columns described the cartesian coordinates of each atom in the structure along with the type of atom. The first column was labeled with the atom's name. The second, third, and fourth columns were labeled with the x, y, and z components of the atom, respectively.

In order to create this list of coordinates that described the shape of the molecules, a material simulator called Materials Studio was used, as used in the previously mentioned studies of Ming Yu [40]. Once Materials Studio was downloaded, oxygen, carbon, and hydrogen atoms were dragged into the space. These atoms were then connected with proper bonds - single, double, or triple, as well as covalent or ionic. The angles between atoms were then changed to match the angles between atoms in the real-life molecule with the angle measuring tool. Once this was done, Materials Studio outputted a list of coordinates of the atoms, which was then sorted according to the type of atom and transferred to the POSITION file. This was done for the estradiol, carbon nanotube, graphene, carbon nanotube with a layer of water, and graphene with a layer of water, leaving a total of five POSITION files.

The second file was KMESH. This file described a mesh that approximated the energy density functional. This functional was used by DFT in its calculations to find the ground state. KMESH has three main lines of code. The first line declared DFT to employ the Monkhorst-Pack method in approximating the electron density functional [23]. The next line contained the vector that describes the amount of k point meshes in each direction. This was set to its default value of <1,1,1> without an increase to reduce the time it took to generate the ground state. The last line of the file contained any shifts in the grid that were needed; however, because no shifts were needed, this was set to <0,0,0>.

The third file was POTENTIAL. The POTENTIAL file contained the pseudopotentials used for each type of atom and was already provided by DFT. Pseudopotentials are an approximation that DFT uses in its calculations of the ground state; it represents the average of all the electrons of an atom in a single electron. Three POTENTIAL files were selected: oxygen, carbon, and hydrogen.

The fourth file was INPUTS, which contained the inputs for the file. The cutoff energy was set at 500 eV [40]. The criteria for the convergence of energy and force in relaxation processes were set to be 10−5 eV and 10−4 eV/Å, respectively [40]. The other inputs were set at the default values.

These files were then submitted into DFT. DFT relaxed the five binary structures and calculated the energies of the systems. Once these binary files were relaxed, DFT outputted the total energy in a file and the relaxed structures in another file. These relaxed structures were uploaded in Materials Studio to ensure no breaks in the structure. New input files were created if breaks were found. The total energies for each molecule were recorded to use for the absorbency energy calculations.

3. Obtaining the Energy of the System

Once the binary structures relaxed, systems were created that contained a nanomaterial and the pharmaceutical. This was done in Materials Studio. After opening the application, a relaxed file of the nanomaterial and estradiol was opened. Then, each structure was copied and pasted onto a new file. Using functions on Materials Studio, the orientation of the pharmaceutical with respect to the nanomaterial was changed to match three different angles, mimicking the diversity of real-life interactions.

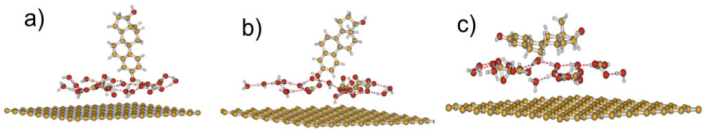

Figure 3. Three Different Orientations. A, B, and C show a vertical orientation, angled orientation, and parallel orientation of the pharmaceutical, respectively. In A, estradiol was positioned to make a 90-degree angle with the surface of graphene or the tangent to the carbon nanotube. In B, estradiol was positioned to make a 45-degree angle with the surface of graphene or the tangent to the carbon nanotube. In C, estradiol was positioned to be parallel to the surface of graphene or the tangent to the carbon nanotube.

Furthermore, the distance between the nanomaterial and the pharmaceutical was set to 1.3 Armstrong units, controlling the position. Once these systems were created, the coordinates of the atoms were once again sorted and inputted into a POSITION file. After these POSITION files were created, the other three input files were created and submitted into DFT. Once the systems were relaxed, the system's energy was recorded, and the images of the pre and post-relaxation structures were recorded.

4. Energy Calculations

The total energies of the tube, graphene, estradiol, and the systems were then used to calculate the absorbency energies. The absorbency energies were calculated by hand with the following equation when there was no water layer between the nanomaterial and pharmaceutical:

$$E(\text{absorption}) = E(\text{System}) - E(\text{Nanomaterial}) - E(\text{Drug})$$

When there was a layer of water between the nanomaterial and pharmaceutical, the following equation was used:

$$E(\text{absorption}) = E(\text{System}) - E(\text{Nanomaterial} + \text{water}) - E(\text{Drug})$$

The total energy of the system was obtained from the system relaxation. Then, each of the total energies of the components from the molecule relaxation was subtracted from the energy obtained from the system relaxation. For instance, to find the absorption energy between the carbon nanotube and estradiol system, the energy of the carbon nanotube and the energy of estradiol after the molecule relaxation were subtracted from the energy of the carbon nanotube and estradiol system after the system relaxation.

Data Analysis

Processes 1- 4 were repeated twice: without a layer of water placed between the nanomaterial and the pharmaceutical and with a layer of water in between. The absorbency measures were analyzed in the statistical program R. Once the excel files were uploaded onto R, the standard deviations and averages were calculated for each of the two sets of data for each nanomaterial. These averages were then represented on a bar graph with error bars representing the standard deviation. Then, a Welch t-test with two degrees of freedom was performed, and t values above the critical value of 3.182 indicated a great enough difference between the absorbency measures to determine that one nanomaterial was significantly more effective at removing the pharmaceutical.

RESULTS & DISCUSSION

	Graphene	Estradiol Molecule	Graphene with 70 H2O Molecules
E_{total} (electron volts)	-907.49345	-265.98271	-324.1844

Table 1. Energy After the Graphene Molecules Were Relaxed. These total energies were obtained after the molecule relaxation. The graphene had 70 water molecules. These were used in the absorbency energy calculations in the final step of the methodology.

	Carbon Nanotube	Estradiol Molecule	Graphene with 70 H2O Molecules
E_{total} (electron volts)	-1158.7441	-265.98317	-2188.8027

Table 2. Energy After the Carbon Nanotube Structures Were Relaxed. These total energies were obtained after the molecules were relaxed. There were 70 water molecules surrounding the carbon nanotube. These were used in the absorbency energy calculations in the final step of the methodology.

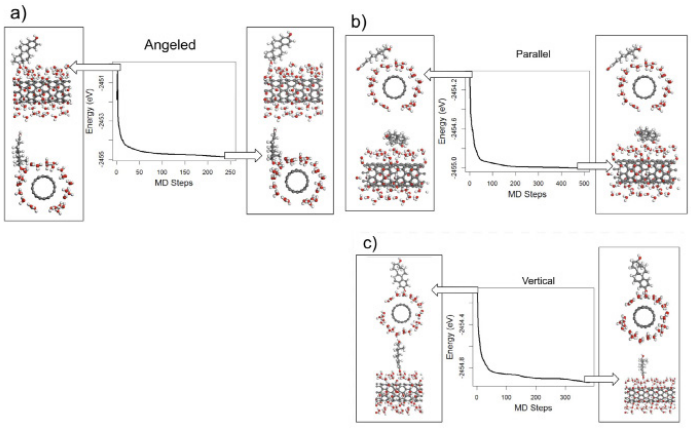

Figure 4. Energy During the System Relaxation Structures and Pre and Post-Relaxation Structures. The asymptote that the line approaches represents

the energy of the ground state for the system, and this value was recorded for the absorbency energy calculations.

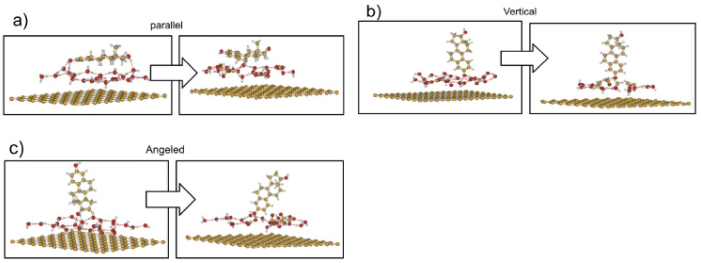

Figure 5. Pre and Post Relaxation Structures for Graphene

Figures 4 and 5 show the structure from before the relaxation process and after the relaxation process. The pre-relaxation structure is an indication of the structure of the carbon nanotubes, and graphene was not damaged or changed by estradiol, ensuring the reusability of the nanomaterials.

Configuration	Carbon Nanotubes	Graphene
Parallel	$E_{absorption}$=0.63 eV	$E_{absorption}$=0.56 eV
Perpendicular	$E_{absorption}$=0.57 eV	$E_{absorption}$=0.49 eV
Angled	$E_{absorption}$=0.58 eV	$E_{absorption}$=0.46 eV
Average	$E_{absorption}$=0.59 eV	$E_{absorption}$=0.50 eV
Standard Deviation	0.03 eV	0.05 eV

Table 3. Absorbency Measures for Carbon Nanotubes vs. Graphene Without Layer of Water. All measurements were in electron volts.

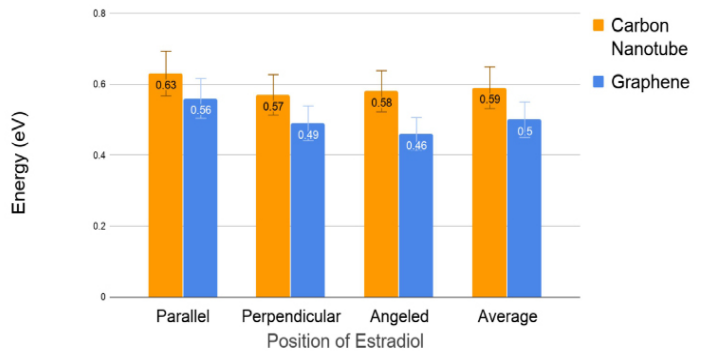

Figure 6. Absorbency Measures for Carbon Nanotubes vs. Graphene Without Water Layer.

Table 3 and Figure 6 show the absorbency energies without a layer of water between estradiol and the nanomaterial. This was done to determine whether there were any interactions between estradiol and the nanomaterial in the dry environment. The absorbency energies for all carbon nanotubes and graphene orientations indicated that strong physical bonds formed between the nanomaterial and pharmaceutical as all absorbency energies were between -0.4 and -0.8 electron volts. The absorbency energies of carbon nanotubes and graphene were between -0.58 to -0.63 and -0.46 to -0.56 electron volts, respectively. The strong physical bonds meant that there were strong attractions between the nanomaterial and estradiol. Additionally, the absorbency energies did not indicate chemical bonds because none of the absorbency measures were above -1.0 electron volts, indicating that neither the carbon nanotubes nor the graphene formed chemical bonds with estradiol and could be reused. A Welch t-test with two degrees of freedom was performed on this data. The t value of 2.53 was less than the critical value of 3.18, indicating that the difference in absorbency energies was not significant.

Configuration	Carbon Nanotubes	Graphene
Parallel	$E_{absorption}$=0.15 eV	$E_{absorption}$=0.48 eV
Perpendicular	$E_{absorption}$=0.15 eV	$E_{absorption}$=0.46 eV
Angled	$E_{absorption}$=0.16 eV	$E_{absorption}$=0.45 eV
Average	$E_{absorption}$=0.1533 eV	$E_{absorption}$=0.4633 eV
Standard Deviation	0.01eV	0.0173 eV

Table 4. Absorbency Measures for Carbon Nanotubes vs. Graphene with Layer of Water

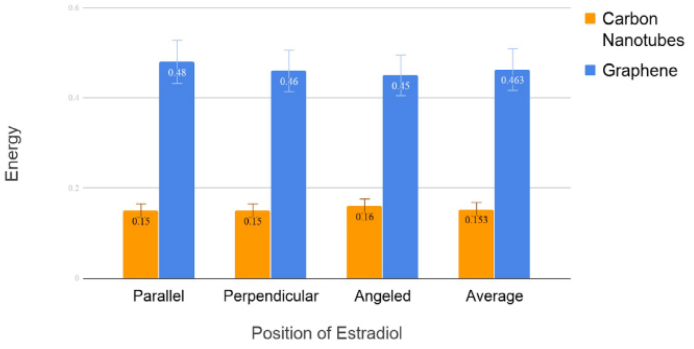

Figure 7. Absorbency Measures for Carbon Nanotubes vs. Graphene with Water Layer.

Table 4 and Figure 7 show the absorbency energies after a layer of water was added between estradiol and the nanomaterial to simulate the water environment. After adding a layer of water between the nanomaterial and pharmaceutical, the average absorbency energy of the carbon nanotubes decreased by 0.45 electron volts, while the average absorbency energy of the graphene decreased by 0.05 electron volts. The ranges of absorbency energies for the graphene and carbon nanotubes

were between -0.45 to -0.48 and -0.15 to -0.16, respectively. The range of absorbency energies for the graphene continued to remain in the interval of strong physical bonds even within an aqueous environment, indicating the graphene could remove estradiol effectively from water. The absorbency energies of the carbon nanotubes decreased to the range of weak physical bonds, indicating that the carbon nanotubes did not have strong enough interactions with the pharmaceuticals for them to be attracted to the filter, making them ineffective. A Welch t-test with two degrees of freedom was performed on this data. The t value of 29.19 indicated a significant difference between the absorbency energies of the carbon nanotubes and graphene.

CONCLUSION

The first phase of the experiment, which was conducted when a water layer was not present, was meant to determine if the interactions between the nanomaterials and the pharmaceutical indicated that both nanomaterials were suitable to be used as a filter. Both materials had strong physical bonds at all three orientations. Thus, the bond did not damage either nanomaterial, allowing them to be reused, and the material effectively attracted estradiol. Therefore, the absorbency energies and structures showed that both nanomaterials have potential in water filtration.

For the second purpose, a layer of water was added to simulate real conditions. The data suggested that graphene could remove estradiol from water and was significantly more effective at removing estradiol from water compared to the carbon nanotubes. Graphene showed great promise in removing pharmaceuticals from water, and the absorbency energies continued to indicate strong physical bonds for graphene. On the other hand, carbon nanotubes had weak physical bonds. These weak physical bonds indicated that when placed in water, the carbon nanotubes would not be able to attract the pharmaceutical to remove it from water.

Furthermore, strong physical bonds for graphene indicated that there is a great enough attraction between the pharmaceutical and nanomaterial for the nanomaterial to remove the pharmaceutical from water but low enough for the pharmaceutical to be easily removed from the nanomaterial without causing permanent damage. Chemical bonds would have drastically increased both the costs and inefficiency of the nanomaterial in removing estradiol from water because chemical bonds are irreversible, so the materials would have to be replaced frequently to counteract the damage.

However, the new understanding is limited. First, the study only tested one pharmaceutical. Although estradiol has a similar shape to many other steroids, there are a variety of different shapes and functional groups that pharmaceuticals can have. Functional groups on the end of pharmaceuticals change the behavior of the pharmaceutical. In the future, more tests can be conducted to ensure that graphene has a high enough absorbance energy to remove various other pharmaceuticals from water.

Moreover, this study only provides a theoretical understanding of the nanomaterials' behavior. The simulation neglects other factors that may decrease the ability of graphene to remove pharmaceuticals from water. For instance, the simulation does not take into account other contaminants in the water supply that may interact with graphene and the pharmaceutical. However, DFT has been perfected by many scientists, and the theoretical understanding provides a basis for the real-life interaction between the nanomaterial and pharmaceutical.

Using the findings of this study, engineers can develop more effective water filters utilizing graphene to remove pharmaceuticals at acceptable rates. Because graphene can be mass-produced and is an abundant element, water filters using graphene as a base would be less costly and, therefore, more accessible. This water filter would potentially eliminate the harms of pharmaceuticals in aquatic environments, treat wastewater from healthcare facilities, and prevent the possible adverse health impacts of pharmaceuticals in the water supply.

ACKNOWLEDGEMENTS

We would like to thank our mentor at the University of Louisville, Dr. Ming Yu, for allowing us to use her lab space and necessary computational tools for our project. We would also like to thank our teachers, Mr. Zwanzig and Mrs. Fries, for guiding us through the research process.

REFERENCES

[1] Alias, N., Musa, H., Sergey, V. R., Hamzah, N., & Al-Rahmi, W. (2017). Nanotechnology theory used for simulation of emerging big data systems on high performance computing: A conceptual framework. *Journal of Theoretical and Applied Information Technology*. 95. 6147-6162. Retrieved from https://www.researchgate.net/publication/321888822_Nan otechnology_theory_used_for_simulation_of_emerging_big_data_systems_on_high_performance_computing_A_conceptual_framework.

[2]Al-Khateeb, L. A., Almotiry, S., & Mohamad, A. S. (2014). Absorption of Pharmaceutical Pollutants onto Graphene Nanoplatelets. *Chemical Engineering Journal*, 248, 191-199. http://dx.doi.org/10.1016/j.cej.2014.03.023.

[3]Amim, M. T., Alazba, A. A., & Manzoor, U. (2014). A Review of Removal of Pollutants from Water/Wastewater Using Different Types of Nanomaterials. *Advances in Material Science and Engineering*, 2014, 1-24. http://dx.doi.org/10.1155/2014/825910.

[4]Anjum, M., Miandad, R., Waqas, M., Gehany, F., & Baraket, M. A. (2016). Remediation of Wastewater Using Various Nanomaterials. *Arabian Journal of Chemistry*. https://doi.org/10.1016/j.arabjc.2016.10.004.

[5]Associated Press. (2008). Drugs in water affect 46 million in the U.S. *NBC News*. Retrieved from http://www.nbcnews.com/id/26662637/ns/health-health_care/t/million-us-have-drugs-drinking-water/#.XIfOmy3MxmA.

[6] Bagheri, H., Afkhami, A., & Noroozi, A. (2016). Removal of Pharmaceutical Compounds from Hospital Wastewaters Using Nanomaterials: A Review. Analytical and Bioanalytical Chemistry Research, 3(1), 1-18. https://pdfs.semanticscholar.org/5896/d61857325d8a79e3861f8ce4d2f07ad52dcf.pdf

[7]Basheer, A. A. (2018). New generation nano-adsorbents for the removal of emerging contaminants in water. *Journal of Molecular Liquids*, 261, 583-593. https://doi.org/10.1016/j.molliq.2018.04.021.

[8] Benotti, M. J., Trenholm, R. A., Vanderford, B. J., Holady, J. C., Stanford, B. D., & Snyder, S. A. (2009). Pharmaceuticals and Endocrine Disrupting Compounds in U.S. Drinking Water. Environmental Science and Technology, 43(3), 597-603. doi: 10.1021/es801845a

[9]Charitidis, A. C., Georgiou, P., Koklioti, M. A., Trompeta, A., & Markakis., V. (2014). Manufacturing Nanomaterials: From Research to Industry. *Manufacturing Review*, 1, 1-11. Doi: 10.1051/mfreview/2014009

[10]Chungsying, L., & Su, F. (2007). Absorption of Natural Organic Matter By Carbon Nanotubes. *Separation and Purification Technology*, 58(1), 113-121. Retrieved from https://www.sciencedirect.com/science/article/pii/S1383586607003218.

[11]Cizmas, L., Sharma, V. K., Gray, C. M., & McDonald, T. J. (2015). Pharmaceuticals and Personal Care Products in Waters: Occurrence, Toxicity, and Risk. *Environmental and Chemistry Letters*, 13(4), 381-394. https://dx.doi.org/10.1007%2Fs10311-015-0524-4.

[12]Cotruvo, J., Couper, M., Cunliffe, D., Fawell, J., Giddings, M., Ohanian, E., … & Simizaki, D. (2011). *Public Health and Environmental Water, Sanitation, Hygiene, and Health: Pharmaceuticals in Drinking Water*. Retrieved from http://www.who.int/water_sanitation _health/publications/2011/pharmaceuticals_20110601.pdf.

[13]Czech, B., & Buda, W. (2015). Photocatalytic treatment of pharmaceutical wastewater using new multiwall-carbon nanotubes/TiO2/SiO2 nanocomposites. *Environmental Research*, 137, 176-184. doi: 10.1016/j.envres.2014.12.006.

[14]Hafner, J. (2008). Ab-initio simulations of materials using VASP: Density-functional theory and beyond. *Computational Solid State Chemistry*, 29(13), 2044-2078. https://doi.org/10.1002/jcc.21057.

[15]Harvard Health Letter. (2011). Drugs in the water. *Harvard Health Publishing*. Retrieved from https://www.health.harvard.edu/newsletter_article/drugs-in-the-water.

[16]Kim, H., Choi, K., Baek, Y., Kim, D. G., Shim, J., Yoon, J., & Lee, J. C. (2014). High performance reverse osmosis CNT/polyamide nanocomposite membrane by controlled interfacial interactions. *ACS Applied Material Science*, 6(4), 2819-2829. Doi: 10.1021/am405398f.

[17]Kim, H., Hwang, Y. S., & Sharma, V. K. (2014). Absorption of antibiotics and iopromide onto single walled and multi walled carbon nanotubes. *Chemical Engineering Journal*, 255, 23-27. Doi: 10.1051/mfreview/2014009

[18]Kohn, W., & Sham, L. J. (1965). Self Consistent Equations Including Exchange and Correlation Effects. Physical Review, 140(4A), 1133 - 1138. http://users.wfu.edu/natalie/s15phy752/lecturenote/KohnPhysRev.140.A1133.pdf

[19]Kresse,G., Marsman, M., & Furthmuller, J. (n.d.). VASP the Guide. Retrieved from https://cms.mpi.univie.ac.at/vasp/vasp/vasp.html.

[20]Lam, S. (2014). Health Effects of Pharmaceuticals in the Water Supply: A Knowledge Synthesis. Retrieved from http://www.ncceh.ca/sites/default/files/Guelph-Lam-2014.pdf.

[21]Leung, H. W., Jin L., Wei, S., Tsui, M. M., Zhou, B., Jiao, L., … & Lam P. K. (2013). Pharmaceuticals in Tap Water: Human Health Risk Assessment and Proposed Monitoring Framework in China. Environmental Health Perspective, 121(7), 839-846. doi: 10.1289/ehp.1206244.

[22]Martin, J. S., May, S., Mebberson, N., Pendleton, P., Krasimir, V., Plush, S. E., & Hayball, J. D. (2017). Activated Carbon, Carbon Nanotubes and Graphene: Materials and Composites for Advanced Water Purification. *Journal of Carbon Research*, 3(18), 1-29. Retrieved from https://res.mdpi.com/carbon/carbon-03-00018/article_deploy/carbon-03-00018.p df?filename=&attachment=1.

[23]Monkhorst, H. J., & Pack, J. D. (1976). Special points for Brillouin-zone integrations. Physics Review, 13(12), 5188-5198. Doi: https://doi.org/10.1103/PhysRevB.13.5188

[24]Narayan, R. (2013). Use of Nanomaterials in Water Purification. *materialstoday*, 13(6), 44-46. Retrieved from https://doi.org/10.1016/S1369-7021(10)70108-5.

[25]Qu, X., Alvarez, P. J., & Li, Q. (2013). Applications of nanotechnology in water and wastewater treatment. *Water Research*, 47(12), 3931-3946. Retrieved from https://www.sciencedirect.com/science/article/abs/pii/S0043135413001772.

[26]Schwarzenbach R. P., Gschwend, P. M, & Imboden, D. M. (2003) Environmental Organic Chemistry Second Edition. New York City, New York: Wiley.

[27]Singh, R. K., Patel, K. D., Kim, J. J., Kim, T. H., Kim, J. H., Shin, U. S., Lee, E. J., Knowles, J. C., & Kim, H. W. (2014). Multifunctional Hybrid Nanocarrier: Magnetic CNTs ensheathed with mesoporous silica for drug delivery and imaging system. *ACS Applied Material Science*, 6(4), 2201-2208. Doi: 10.1021/am4056936.

[28]Sun, G., Kurti, J., Rajcyz, P., Kertesz, M., Hafner, J., & Kresse, G. (2003). Performance of the Vienna ab initio simulation package (VASP) in chemical applications. *Journal of Molecular Structure*, 624, 37-45. http://karin.fq.uh.cu/~lmc/ref/old/sun03.pdf

[29]Thamaraiselvan, C., Lerman, S., Weinfeld-Cohen, K., & Dosoretz, C. G. (2018). Characterization of a support-free carbon nanotube-microporous membrane for water and wastewater filtration[abstract]. *Separation & Purification Technology*, 202, 1–8. https://doi.org/10.1016/j.seppur.2018.03.038.

[30]Tijani, J. O., Fatoba, O. O., & Petrik, L. F. (2013). A Review of Pharmaceuticals and Endocrine-Disrupting Compounds: Sources,Effects, Removal, and Detections. *Water Air Soil Pollut*,

224(1770), 1-29. doi: 10.1007/s11270-013-1770-3.
[31]Upadhyayula, V. K., Deng, S., Mitchell, M. C., & Smith, G. B. (2009). Application of Carbon Nanotube technology for the removal of contaminants in drinking water: a review. *Science Total Environment*, 408(1), 1-13. Doi: 0.1016/j.scitotenv.2009.09.027
[32]Wang, Y., Wang, W., Li, M., Dong, J., & Chen, G. (2018). Removal of Pharmaceutical and Personal Care Products from Municipal Wastewater with Integrated Membrane Systems, MBR-RO/NF. *International Journal of Environmental Research and Public Health,* 15(2), 269. https://doi.org/10.3390/ijerph15020269.
[33]Wang, Y., Wang, W., Li, M., Dong, J., & Chen, G. (2018). Removal of Pharmaceutical and Personal Care Products from Municipal Wastewater with Integrated Membrane Systems, MBR-RO/NF. *International Journal of Environmental Research and Public Health*, 15(2), 269. https://doi.org/10.3390/ijerph15020269.
[34]WebMD. (n.d.). Estradiol. *WebMD*. Retrieved from https://www.webmd.com/drugs/2/drug-5186/estradiol-oral/details
[35] Westerhoff, P., Alvarez, P., Li, Q., Torresdey, J. G., & Zimmerman, J. (2016). Overcoming implementation barriers for nanotechnology in drinking water treatment. *Environmental Science Nano*, 3, 1241-1253. doi: 10.1039/C6EN00183A.
[36] Xu, P., Zeng, G. M., Huang, D. H., Feng, C. L., … & Liu, Z. F. (2012). Use of Iron Oxide Nanomaterials in Wastewater Treatment. Science of the Total Environment, 424, 1-10. Retrieved from https://doi.org/10.1016/j.scitotenv.2012.02.023.
[37] Xu, J., Cao, Z., Zhang, Y., Yuan, Z., Lou, Z., Xu, X., & Wang, X. (2018). A review of functionalized carbon nanotubes and graphene for heavy metal adsorption from water: Preparation, Application and mechanism. *Chemosphere*, 195, 351–364. https://doi.org/10.1016/j.chemosphere.2017.12.06
[38]Yang, G. C. C., & Yen, C.-H. (2013). The use of different materials to form the intermediate layers of tubular carbon nanofibers/carbon/alumina composite membranes for removing pharmaceuticals from aqueous solutions[abstract]. *Journal of Membrane Science*, 425–426, 121–130. https://doi.org/10.1016/j.memsci.2012.09.011.
[39] Zaib, Q., Mansoor, B., & Ahmed, F. (2013). Photo-regenerable multi-walled carbon nanotube membranes for the removal of pharmaceutical micropollutants from water. *Environmental Science Process Impacts*, 15(8), 1582-1589. doi: 10.1039/c3em00150d.
[40]Zhang, C., Yu, M., Anderson, G., Dharmasena, R. R., & Sumanasekera, G. (2017). The prospects of phosphorene as an anode material for high-performance lithium-ion batteries: a fundamental study. *Nanotechnology*, 28, 1-19. doi:10.1088/1361-6528/aa52ac.
[41]World Health Organization. (2012). Pharmaceuticals in Drinking Water. *World Health Organizations.* Retrieved from https://apps.who.int/iris/bitstream/handle/10665/44630/9789241502085_eng.

Curcumin Improves Human Islet Insulin Secretion and Viability by Reducing Oxidative Stress

Dharshini Kumar[1]
[1]**duPont Manual High School**
Louisville, Kentucky

Mentor: Bala Appakalai, Cardiovascular Innovation Institute

ABSTRACT

Type 1 diabetes has affected millions of children worldwide, and they typically must take daily insulin injections and multiple blood glucose level tests. With recent advancements, a new treatment to cope with Type 1 diabetes has been developed: islet cell transplants. This treatment provides the diabetic patient up to 10 years of being diabetes-free before the islet cell returns to a diabetic state. This return is due to the presence of islet isolation stress on the cells. This stress is composed of external and oxidative stress received from the cell removal process. Isolation stress results in poor function, which ultimately results in cell death. To combat this stress, a powerful antioxidant must be used to improve insulin secretion and islet viability. This could be done by cultivating the cells with the compound curcumin, which has a powerful antioxidant property. First, the optimum dosage of curcumin was determined (20 micromolar) and was used consistently throughout experimentation. Next, islet viability and recovery were calculated from 10 pancreases. Afterwards, the oxidative stress, antioxidant enzymes, and antioxidant molecules were measured. Following this, a Glucose-Perifusion Assay was performed along with an Insulin ELISA to determine insulin secretion for high and low glucose levels. Lastly, a reversal of diabetes in a nude mice model was performed. In each analysis, the experimental group provided beneficial effects to the islet cells. Thus, the culturing of islet cells in curcumin did reduce oxidative stress, which improved insulin secretion and cell viability.

INTRODUCTION

Diabetes

Diabetes is defined as the lack of insulin in the bloodstream. Therefore, people with diabetes regularly take insulin shots to break down the food in their body and provide energy for their cells (Association, 2000). In Type 1 diabetes, the human body is unable to produce insulin because the insulin-producing cells are destroyed. This type of diabetes has affected millions of children worldwide, with approximately 1,250,000 in America alone ("Diabetes Prevalence," 2018). With recent medical advancements, there is an option that has allowed them to have a transplant for new islet cells. These islet cells are located in the pancreas and help produce insulin in order to get the nutrients from food. For a person to develop diabetes, the islet cells are attacked by their immune system because it believes the cells are foreign. The patient then must take insulin at least three times a day so that the food can be converted into nutrients for the different cells in the body. Islet cells are the beta cells of the islets of Langerhans (National Institute of Diabetes, 1999). This term is interchangeable with islet cells.

Role of Insulin

Insulin is secreted by the beta cells of islets of Langerhans, and secretion is triggered by elevated glucose concentration in the blood. Normal insulin secretion for a healthy individual 30 minutes after a meal is 30-230 mIL/U (multi-International Liters per unit). This insulin is used to "signal muscle, fat, and liver cells in the body to absorb glucose (sugar) from the bloodstream to be used for energy...[and signal] the liver to stop releasing glucose into the bloodstream" (Campbell, 2018). Insulin plays a vital role in the function of the human body by providing nutrients to replenish the body from daily functions.

Islet Cell Transplant

Islet cell transplantation, a medical treatment in which lost islet cells are replaced by providing the patient with new islet cells from a donor, has recently been developed as a treatment for patients with Type 1 diabetes (American Diabetes Association, 2006). Now, patients have the option to get this transplant, which would provide them at least ten years of being diabetes-free before the cells return to a diabetic state (Williams et al., 2018).

Islet cells sustain a considerable amount of stress during the process of collection from the donor's pancreas. The cells are removed from their regular habitat, which can essentially put a timer on them (Qi et al., 2009a). Stress from the isolation process impacts the islet cells, enzyme digestion, and the centrifuge's ability to collect the cells, causing them to underperform. When implanted in a new patient, this underperformance could ultimately lead to cell death. There have been recent improvements in the islet isolation procedure, which include using highly purified collagenase, an enzyme used to breakdown the pancreas, in conjunction with thermolysin or neutral protease, followed by purification with continuous density gradients. This yielded an improvement in islet quantity, which in turn improved the application of low-doses of immunosuppressants to prevent allograft rejection, and most importantly, increased attention to proper post-transplant management (Buchwald & Cechin, 2013). The use of immunosuppressive drugs in the islet cell transplant was used to eliminate the possibility of rejection in the patient's body. However, this usage caused more stress on these islet cells, as they were being suppressed into working for a foreign host (Bertuzzi & Carlis, 2016).

Reactive Oxygen Species and Free Radicals

The National Cancer Institute defines reactive oxidative species as "a type of unstable molecule" containing oxygen. This molecule reacts with other molecules in the cell, which can cause damage to DNA, RNA, and proteins and may cause cell death (2018). The reactive oxygen species that come about in islet cells are found in the mitochondrial respiratory chain. Free radicals commonly occur in the "presence of an unpaired electron" (Lobo et al., 2010). They are known to attack the macromolecules located within the cell, which leads to cell damage and the disruption of homeostasis. Homeostasis is defined as the ability to maintain a constant internal environment, even when the outside environment is changing.

Philipp A. Gerber from the University of Zurich and Guy A. Rutter, a professor of cell biology and functional genomics, revealed that there are multiple stimulations from simple tasks of the islet cells that cause the formation of reactive oxygen species (ROS), including converting glucose and fatty acids (2017). These numerous tasks can lead to an abundance of ROS, which causes oxidative stress. This oxidative stress would, in turn, cause lipid peroxidation, which is "the oxidative degradation of lipids" (Gutowski & Kowalczyk, 2013). This means damage to the cellular membrane will occur because the membrane is made up of lipids. The process of lipid peroxidation follows after free radicals start to accumulate.

Ramon Rodrigo, a professor of biology in the Institute of Biomedical Sciences Faculty of Medicine at the University of Chile, explicitly describes the effect of oxidative stress on the cells located in the cardiovascular system. Many cells within this system go through the same processes as islet cells in the pancreas, which gives an accurate comparison of the oxidative stress that both cells would receive. Oxidative stress, as defined by Rodrigo, "is an imbalance between pro-oxidants and antioxidants." This imbalance is created from the normal rate and magnitude of oxidant formation being more than the rate of oxidant elimination (2009). This can cause an increase in ROS levels, and since they are radicals that possess an unpaired electron, it "makes them highly reactive and thereby able to damage all macromolecules, including lipids, proteins, and nucleic acids" (Bowen, n.d.).

Omolola R. Ayepola and colleagues from the Department of Biochemistry at the Stellenbosch University conducted a study examining the relationship between oxidative stress and diabetic complications. Ayepola found that "in the onset and progression of late diabetic complication[s], free radicals have got a major role due to their ability to damage lipids, proteins and DNA" (2014). This damage can be extremely dangerous for any cell because it can lead to cell death.

Curcumin

Curcumin, a bright yellow compound used in numerous traditional Indian medicines and dishes, is being used more frequently in modern-day medicine. It has several properties that can be utilized in numerous medications, such as antibacterial, antioxidant, and antimicrobial medications (Gupta et al., 2012). With the discovery of its properties, there have been numerous clinical trials conducted with curcumin. Ak & Gülçin from Ataturk University tested the antioxidant properties of curcumin on lipid peroxidation damage done to liver cells. They found that it was extremely beneficial in reducing this damage (2008). Since curcumin can act as a powerful antioxidant, this study showed that curcumin is able to reduce the stress occurring during islet cell transplants. This specific stress is the oxidative stress that has built up due to the isolation and removal process.

Presently-Used Drugs

Today, glucagon-like peptide 1 (GLP-1) is being used to prevent cell death after a patient has received a transplant. This drug helps with "the regeneration of beta cells, protection of those cells against apoptosis (programmed cell death), enhancement of insulin secretion after meals, and suppression of the release of glucose from the liver after meals" (Dinsmoor, 2006). While patients can take drugs that have GLP-1, there are many associated safety concerns. These concerns include damage to the patient's liver, pancreas trouble with regards to immunity, and lack of islet function. Because of these safety concerns, islet cells that were given to the patient may be harmed, leading to increased cell death. This increase in cell death will severely impact the patient because there is typically a limited amount of islet cells that can be given to the diabetic patient. If curcumin is shown to prevent islet cell death, it can be a safer alternative to the aforementioned drug.

Previous Research

In 2017, a project was conducted to test whether there was an effect on insulin production with the presence of curcumin. The results showed that the cultivation of islet cells with curcumin showed a great improvement in their ability to produce insulin. The null hypothesis of this experiment, which was that curcumin would affect insulin production, was supported by the results because the treated group performed everyday functions better than the control group.

Present Research

The following research aims to improve this procedure because about 20-30% of islet cells from a donor pancreas are lost from the beginning stages of the isolation procedure alone. More islet cells are lost than given to the diabetic patient, and many cells that are scavenged from the donor are severely damaged from the buildup of free radicals. These free radicals cause oxidative stress in islets, which can cause increased cell death. The incorporation of a beneficial compound to prevent or reduce this oxidative stress would benefit these islet cells and lead to an extension of the treatment. The hypothesis for this study is that reducing islet cell stress during the culturing process will improve islet viability and function.

METHODOLOGY

This study utilized a true experimental quantitative method. Within the background research conducted, a similar study was found, and it explored how to see the improvement of oxidative stress in islet cells by inducing the cells with a variable. Manisha Modak and colleagues from Sri Parshurambhau College conducted a study focused on whether controlling hyperglycemia, a state in which blood glucose is too high, would reduce oxidative stress that occurred in the islet cells (2011). This specific study was chosen as a vital mentor text to perform the research because it also measured oxidative stress in islet cells. There were a total of six methods used in their study that were also used in this research. Along with these six methods, an additional two methods, FDA/PI staining and a Glucose Perifusion Assay, were also conducted to look at improvement in insulin secretion. The islet isolation procedure, which is the standard procedure for extracting islet cells, was also used for this study.

Islet Isolation Procedure

To collect islet cells, the fat from the pancreas was first removed. The pancreas was then split into four sections. In each section of the pancreas, there is a vein, and a valve was inserted into it to apply the cleaning solution. The pancreas was washed thoroughly using collagenase, a cleaning solution and degradation enzyme. This was done to each piece of the pancreas. Next, the pieces were placed into the Ricordi Chamber, the first stress factor of the isolation process. A Ricordi Chamber is used to digest the pancreas so that the islet cells will be easier to collect. The Ricordi Chamber was used manually so that the pressure on the pancreas was not too high.

To digest the pancreas, the Ricordi Chamber must be at 37 degrees Celsius, and the power cannot go over 20. There are tubes on the Ricordi Chamber where the digested pancreas travels down to be collected in separate tubes and sent to the centrifuge. Throughout the process, the digested pancreas was checked on to make sure there were islet cells present. The Dithizone Staining Technique was used for the identification of islet cells. The liquid that was collected from the digestion was a mix of islet cells and dissociated pancreas tissue. Once the pancreas had been fully digested, it was taken to the centrifuge so that the islet cells and the rest of the pancreatic cells could be separated. The digested liquid was placed into tubes to be placed into the centrifuge. This mechanical spinning process was a stress factor for the islet cells.

The tubes were in the centrifuge for approximately 22 minutes. Once the centrifuge step was complete, the tube had the islet cells floating on the top (since they were less dense) and the pancreatic cells at the bottom. The pancreatic cells were then taken out, and the islet cells were put back into the centrifuge and spun for another 3 to 5 minutes.

After the islet cells were collected, they were ready to be cultured. For this study, the islet cells were cultured with curcumin to see if their secretion and viability would improve. The culturing of the islet cells took approximately 48 hours. There were two groups, the experimental or treated, which had the curcumin-culture, and the control, which had islet cells cultured in normal medium.

FDA/PI Staining

This staining technique was used to determine islet viability and recovery. There were two fluorescence stains used to determine whether the islet cell was living or dead. A cell-permeable substrate, fluorescein diacetate (FDA), and a cell impermeant called propidium iodide (PI) are commonly used to determine the viability of the islet of Langerhans cells (Boyd et al., 2008).

Glucose Perifusion Assay

This assay monitors the amount of insulin secreted by the islet cells for high and low glucose levels. It was used to simulate what these islet cells would experience in the human body. The islet cells would be exposed in the order of low, high, and low glucose levels. The insulin secreted was later analyzed with an Insulin ELISA Kit, a specific enzyme-linked immunosorbent assay (ELISA) made to calculate the amount of insulin produced. In the ELISA, a specific anti-insulin antibody was in ninety-six well microtiter plates and would specifically attach to insulin. Thus, the attached insulin would be measured using the technique provided in this kit. This assay was the most common assay conducted for testing islet cells that were ready to be transplanted into diabetic patients.

Antioxidant Enzymes and Molecules

The enzymes used include glutathione reductase, catalase, superoxide dismutase, and glutathione peroxidase. The molecules used were reduced uric acid and reduced glutathione. These enzymes and molecules serve the same function of being a defense for the islet cells against free radicals so that further harm to the cell will be prevented. As stated above, these molecules and enzymes will attack free radicals, but it is hypothesized that if these islet cells are cultured with curcumin, there will be no need for these molecules and enzymes to activate. Thus, if there is an increased amount of enzymes or molecules, that would mean that there are fewer free radicals in the presence of the cell, and the compound may have helped the islet cells.

Estimation of Lipid Peroxidation, Protein Carbonyl, and Amount of 8OHdg

The estimation of lipid peroxidation is the

estimation of damage to the cellular membrane of the islet cell. This damage occurs due to free radicals. In order to monitor this, malondialdehyde (MDA) was used because it is commonly recognized as a biomarker for cellular damage done by free radicals. If there is an increase in MDA, which is determined using thiobarbituric acid (TBA), there are more free radicals, and therefore, more oxidative stress is occurring in islet cells. When TBA reacts with MDA, a bright fluorescent red is observed, showing the amount of MDA (Ayala et al., 2014). The estimation of protein carbonyls is used to see the oxidative damage done to the cells' proteins. If there is an increased amount of the formation of these carbonyls, it will be indicated by more oxidative stress. Lastly, the amount of 8OHdG is an analysis technique used to indicate the oxidative damage to the nuclear DNA of the islet cells. 8-hydroxydeoxyguanosine (8OHdG) is a DNA sequence frequently studied and known as a biomarker for oxidative stress (Wu et al., 2004). If there is an increased amount of this biomarker present in islet cells' nuclear DNA, this will indicate more oxidative stress.

Reversal of Diabetes in Nude Mice Model

The last analysis method used was the nude mice model. In this model, the nude mouse, a specific type of mouse used due to its inhibited immune system, was induced with diabetes using the drug streptozotocin (STZ) to analyze diabetes in a living model. This model will portray the complete reversal of diabetes, showing the return of normal blood glucose levels in these mice. This method simulates what will happen if these islet cells are given to a diabetic patient. This analysis will portray whether these islet cells benefit and function properly inside a diabetic patient. There will be four groups: a nontreated control, which have the human islet cells cultured in normal culture medium, the non-diabetic control, which will model normal blood glucose levels in these mice, the diabetic control, which will model the blood glucose levels of a diabetic mouse, and the experimental group-treated, which have the human islet cells cultured in curcumin. The goal of this is to show the amount of time it takes for the experimental group-treated and nontreated control to reach normal blood glucose levels of those in the non-diabetic control.

Statistical Analysis

Two types of statistical significance tests were run depending on the type of analysis technique being monitored. The two were a student paired t-test (a common statistical test used to compare two groups) and an Analysis of Variance (ANOVA) test, which compares multiple groups to one another to test significance. For the antioxidant molecules and enzymes, estimation in protein carbonyls, estimation in lipid peroxidation, and amount of 8OHdG, a student t-test was run. For the others, an ANOVA test was run. The significance value was P=0.05 for all tests conducted. The graphs that will be displayed in the next section are representations of the average amount of islet cells for each.

RESULTS

The first test conducted aimed to find the optimum dosage of curcumin that would provide the maximum amount of benefits to the islet cells. This was done using four dosage types: 10, 20, 40, and 80 µm. The viability of these cells was measured using the FDA/PI staining method. 20 µm provided the maximum amount of benefits.

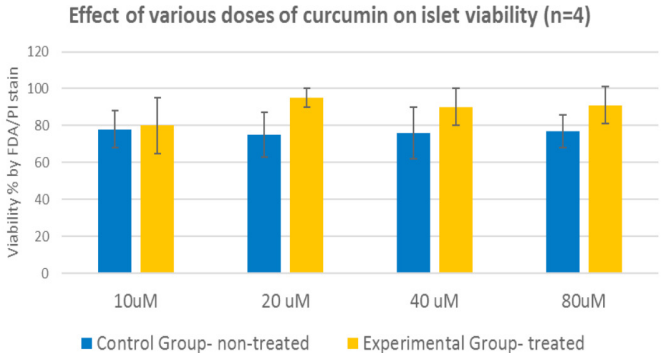

Figure 1. Islet Viability Based on Level of Dose of Curcumin

Next, islet recovery and viability were tested. Islet cells from 10 different pancreases were used. Both used the FDA/PI staining method. Recovery looked at how many of 100 islet cells survived, and viability looked at how many islet cells had survived after the 48-hour culture period.

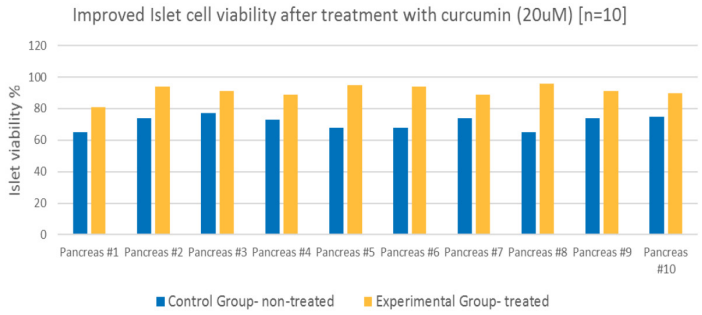

Figure 2. Improved Islet Cell Viability After Treatment With Curcumin (20 UM) [n=10]

As seen above, this graph displays that all experimental groups (curcumin-cultured groups) have significantly higher percentages of islet viability compared to the control group.

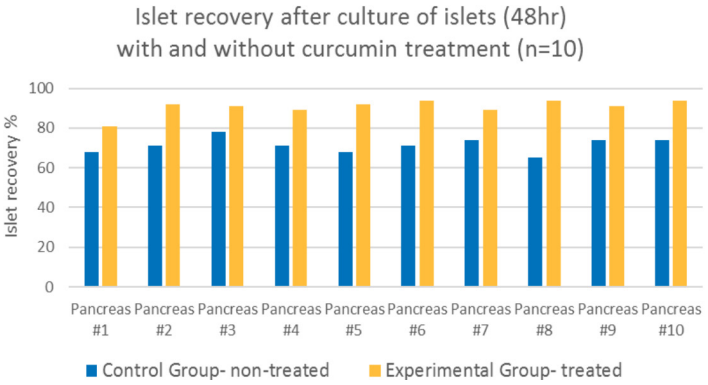

Figure 3. Islet Recovery After Culture of Islets (48hr) With and Without Curcumin Treatment (n=10)

In Figure 3, the recovery percentage of islet cells from a culture of one hundred cells is shown. The approximate amount of islet cells that survived after the 48-hour period can also be gauged above. The experimental groups showed a significantly higher amount of these islet cells than the control group, suggesting that curcumin was increasing islet viability.

After the islet viability and recovery was the estimation of lipid peroxidation that occurred within the cell. The control group seemed to have more lipid peroxidation than the curcumin-cultured islet cells because much of the control group islet cells had sustained damage from the previously stated islet isolation process. Figure 4 shows these results. The amount of damage done to cells in the control was represented by a standard deviation of 29, while that of the experimental group was 21. The mean of lipid peroxidation for the experimental group was 90 µmoles of MDA formed per 100 mg, while the control group was centered around a mean of 174 µmoles of MDA formed per 100 mg. This shows that there was a significant decrease in damage done to the cellular membrane by culturing islet cells with curcumin.

The carbonyl group estimation was performed after and also supported the null hypothesis. Figure 5 displays the means for the control and experimental groups, and there is a considerable gap between the two. The graph shows a significant decrease in carbonyl groups, which are directly correlated with a decrease in oxidative stress. Following protein carbonyl estimation was the analysis of the amount of 8OHdG segment using a competitive ELISA test. The results from this show that there were fewer biomarkers for the free radicals in the curcumin-cultured islet cells compared to the control group of islet cells. The average means of both groups, shown in Figure 6, had a gap of 30 mmoles per microgram/DNA, showing a significant decrease of free radicals in the experimental group.

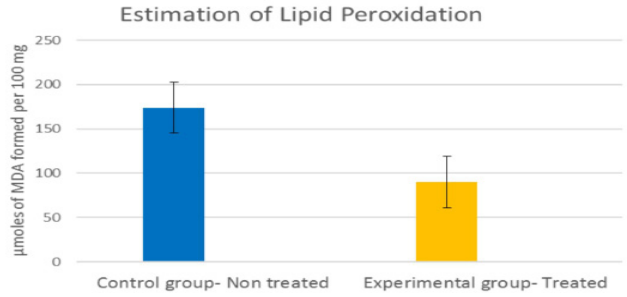

Figure 4. Estimation of Lipid Peroxidation

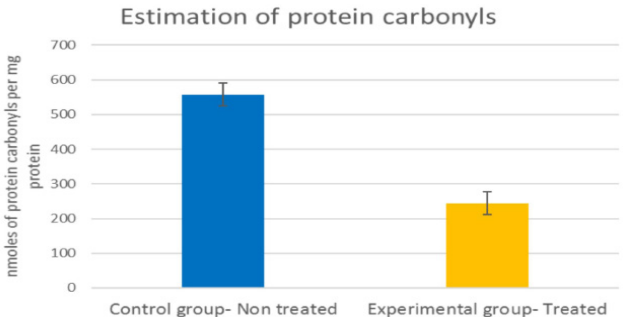

Figure 5. Estimation of Protein Carbonyls

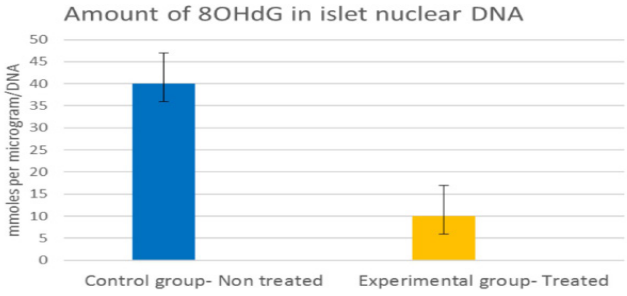

Figure 6. Amount of 8OHdG in Islet Nuclear DNA

Next came the use of the antioxidant molecule reduced glutathione, along with reduced uric acid, and the antioxidant enzymes glutathione reductase, catalase, superoxide dismutase, and glutathione peroxidase. Figures 7.1 through 7.4 (see Appendix) portray the results from the enzymes used, and Figures 8.1 and 8.2 (see Appendix) portray the results from the molecules used. The figures show that the curcumin-cultured cells did have less free radicals and less oxidative stress.

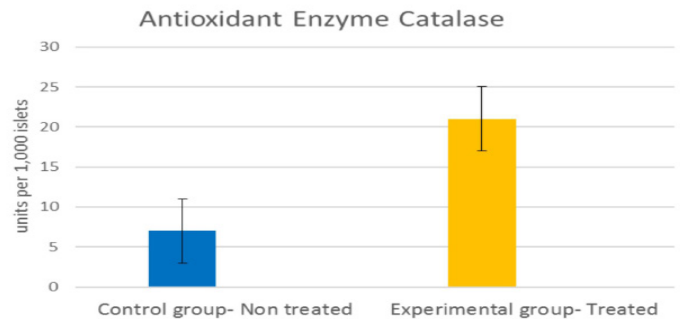

Figure 7.1. Antioxidant Enzyme Catalase

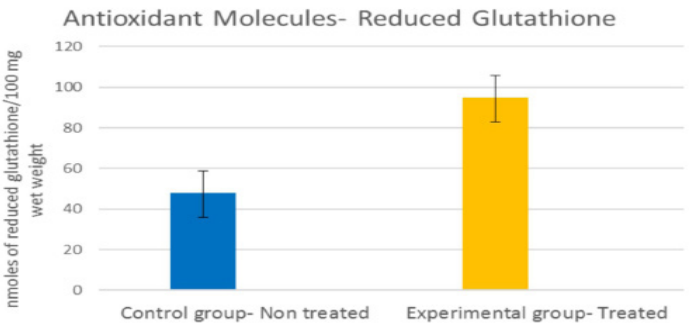

Figure 8.1. Antioxidant Molecule Reduced Glutathione

Next, the Glucose Perifusion Assay was performed. This assay provided results based on high and low glucose levels as a simulation of the human body. The results show that there was a significant improvement in insulin production for islet cells cultured in curcumin than those cultured in a regular culture medium. For the low-glucose concentration, the produced insulin for the treatment groups averaged to about 25 to 30 ulUnit/ml, and for high-glucose exposure, it averaged to about 80 to 100 ulUnit/ml. Both of these averages were higher than that of the control, which averaged to 15 to 20 ulUnit/ml for low glucose levels and 20 to 40 ulUnit/ml for high glucose levels. As seen in Figure 9.1 and Figure 9.2, the insulin release for both high and low glucose levels in the curcumin-cultured cells was significantly higher than those of the regular control.

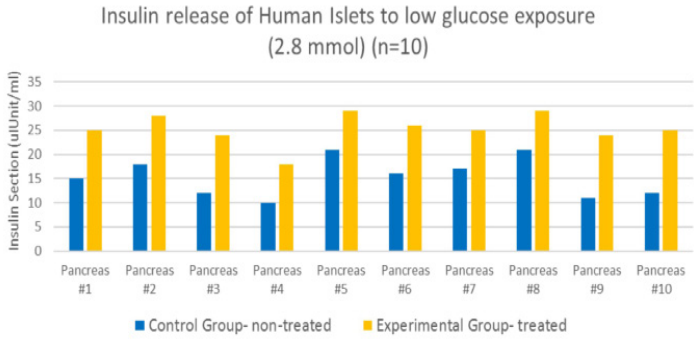

Figure 9.1. Insulin Release of Human Islets to Low Glucose Exposure (2.8mmol) (n=10)

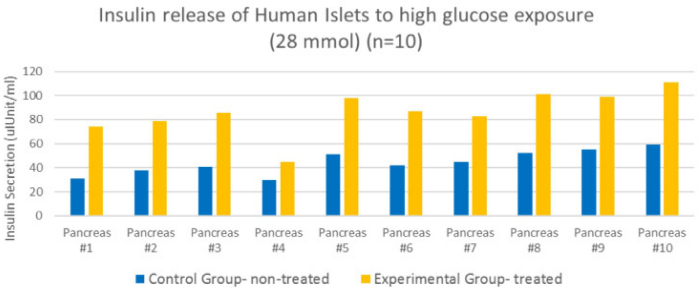

Figure 9.2. Insulin Release of Human Islet to High Glucose Exposure

The reversal of diabetes in a nude mice model portrayed a simulation of how the islet cells would perform if given to humans. Over the course of 30 days of monitoring, the experimental treated group displayed blood glucose levels around 100 mg/dL, which is similar to glucose levels in non-diabetic mice. The control only reached levels lower than 200 towards the end of the 30-day period.

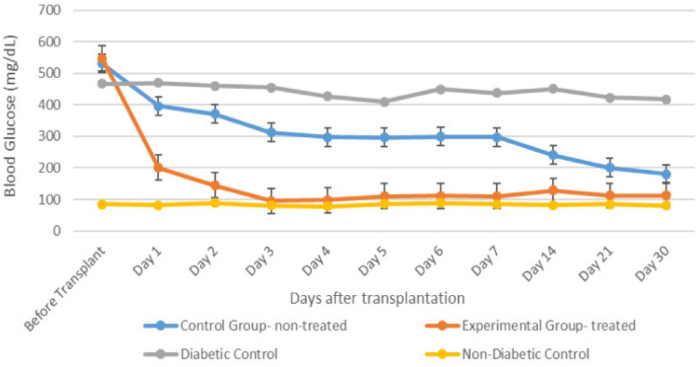

Figure 10. Reversal of Diabetes After Transplantation in Mice Model

DISCUSSION

After determining the optimum dosage of

20 µm of curcumin used in each culture for the experimental groups, the other analysis tests could be started. Islet viability (Figure 2) and recovery (Figure 3) showed that cells cultured with curcumin had increased viability and recovery rates than those cultured with regular medium. Next were the oxidative stress-related analysis techniques. In the estimation of protein carbonyls (Figure 5) and lipid peroxidation (Figure 4), the experimental group showed a significantly low amount of damage compared to the control. The amount of the 8OHdG (Figure 6) was also shown to be a significantly low amount compared to the control. Following these three tests were those of the antioxidant molecules (see Figure 8.1 in Results and Figure 8.2 in Appendix) and enzymes (see Figures 7.1 in Results and Figures 7.2,7.3, and 7.4 in Appendix). All enzymes and molecules were shown in an increased amount, showing that these enzymes and molecules had nothing to defend the cells against.

The Glucose Perifusion Assay was conducted next. In Figure 9.1, the low glucose was tested, and the experimental group was shown to have a significantly increased amount of insulin secretion compared to the control. The same results were shown for Figure 9.2, which tested high glucose on the islet cells. Lastly, the reversal of diabetes in the nude mice model was conducted. Figure 10 shows that the experimental group had the fastest reversal in diabetes compared to the nontreated control group as it reached similar blood glucose levels to that of the non-diabetic control. With these analysis methods, it may be concluded that using the compound curcumin in the culturing step of the isolation process is beneficial to islet cells because it decreases oxidative stress, significantly improving islet viability and insulin secretion.

These analysis methods provided similar results to the study by Modak and others, as there was a significant decrease in oxidative stress by inducing the islet cells with a variable. In their case, it was hyperglycemia (2011). The results have consistently shown that the curcumin-cultured islet cells have performed better and had a reduction in free radicals, preventing any damage to be instigated on the cells and increasing the viability of the islet cells. This increase in cell viability prevented cell death (Rojas et al., 2018) from occurring, which will benefit diabetic patients receiving this treatment.

CONCLUSION

With this knowledge, doctors who are aiming to eradicate diabetes using this type of treatment will be able to provide more islet cells for the islet cell transplants, which will increase the longevity of this treatment. This increase in longevity would be extremely beneficial for Type 1 diabetic patients because they do not need to return to the usage of daily insulin injections after ten years (or less) pass. With the use of curcumin in the culturing period, the overall transplantation process will be impacted profoundly.

FUTURE DIRECTIONS

The research conducted can be used to improve the current isolation and culturing procedures used in islet cell transplantation. With the incorporation of the compound curcumin, there will be a significant increase in islet viability and function, providing better treatment for the patient. This compound can also be used to culture various other cells that experience oxidative stress to improve their function and viability.

A limitation that occurred while conducting this research was choosing the types of methods that could be used in the given time frame. Much of the islet viability and recovery portions were done, and the Glucose Perifusion Assays were underway, but the new methods of analyzing the antioxidant stress were challenging to find. At first, the research aimed to examine oxidative damage done to the DNA of the islet cells and the free radical count. Techniques that would have been used include electron spin resonance, which is somewhat similar to the antioxidant molecules and enzymes, a Deoxyribose Degradation Assay, and a Metmyoglobin Assay. These two assays would look at the damage done to the islet cell DNA. It was not possible to use such techniques because the lab did not have the necessary equipment. Further investigations for different ways to measure oxidative stress were conducted, and the paper by Modak and colleagues provided possible ideas for analysis techniques.

For further research, an improvement could be made in the way the islet cells are collected for islet cell transplants so that the prevention of islet isolation stress will be at the beginning.

Another direction would be to continue this project and implement it in higher living models. This is the next step for many researchers after initial lab testing. Also, this will provide the gateway to using this compound in human islet cell transplants. Along with this, the reduction of the external stress factors that are seen in the isolation process by understanding how to remove islet cells without causing stress early on would be helpful. Therefore, the idea that an anti-stress compound may not be needed is a future goal to address.

ACKNOWLEDGEMENTS

Special thanks to Dr. Balamurugan Appakalai for providing an opportunity to research and study Islet cells and for providing guidance and mentorship throughout the past 3 years. It was truly a privilege to work with you. Thank you to my parents for supporting me through this incredible educational journey.

REFERENCES

Ak, T., & Gülçin, I. (2008). Antioxidant and radical scavenging properties of curcumin. *Chemico-Biological Interactions*, 174(1), 27-37. doi:10.1016/j.cbi.2008.05.003

American Diabetes Association. (2006). Pancreas and Islet Transplantation in Type 1 Diabetes. *Diabetes Care*, 29(4), 935-935. doi:10.2337/diacare.29.04.06.dc06-9908

Antonio Ayala, Mario F. Muñoz, and Sandro Argüelles, "Lipid Peroxidation: Production, Metabolism, and Signaling Mechanisms of Malondialdehyde and 4-Hydroxy-2-Nonenal," Oxidative Medicine and Cellular Longevity, vol. 2014, Article ID 360438, 31 pages, 2014. https://doi.org/10.1155/2014/360438.

Asmat, U., Abad, K., & Ismail, K. (2016). Diabetes mellitus and oxidative stress—A concise review. *Saudi Pharmaceutical Journal*, 24(5), 547-553. doi: 10.1016/j.jsps.2015.03.013

Association, A. D. (2000). Type 2 Diabetes in Children and Adolescents. *Pediatrics*, 105(3), 671-680. doi:10.1542/peds.105.3.671

Ayepola, O.R., Brooks, N.L., Oguntibeju, O.O. 2014. Oxidative Stress and Diabetic Complications: The Role of Antioxidant Vitamins and Flavonoids.

Aziz, M. T., El-Asmar, M., Rezq, A., Wassef, M. A., Fouad, H., Roshdy, N., . . . Hassouna, A. (2014). Effects of a novel curcumin derivative on insulin synthesis and secretion in streptozotocin-treated rat pancreatic islets in vitro. *Chinese Medicine*, 9(1), 3. doi:10.1186/1749-8546-9-3

Bentsi-Barnes, K., Doyle, M. E., Abad, D., Kandeel, F., & Al-Abdullah, I. (2011). Detailed protocol for evaluation of dynamic perifusion of human islets to assess β-cell function. *Islets*, 3(5), 284-90.

Bertuzzi, F., & Carlis, L. G. (2016). Human Pancreatic Islet Production: From Research Protocols to Standardized Multicenter Manufacturing. *Diabetes*, 65(11), 3243-3245. doi:10.2337/dbi16-0045

Betteridge, D. J. (2000). What is oxidative stress? *Metabolism*, 49(2), 3-8. doi:10.1016/s0026-0495(00)80077-3

Boyd, Vinc et al. "Limitations in the Use of Fluorescein Diacetate/Propidium Iodide (FDA/PI) and Cell Permeable Nucleic Acid Stains for Viability Measurements of Isolated Islets of Langerhans" *Current trends in biotechnology and pharmacy vol.* 2,2 (2008): 66-84.

Buchwald, P., & Cechin, S. R. (2013, May 20). Glucose-stimulated insulin secretion in isolated pancreatic islets: Multiphysics FEM model calculations compared to results of perfusion experiments with human islets. Retrieved from https://www.scirp.org/journal/PaperInformation.aspx?PaperID=32031

Bowen, R. (n.d.). Free Radicals and Reactive Oxygen. Retrieved from http://www.vivo.colostate.edu/hbooks/pathphys/topics/radicals.html

Campbell, A. (2018). What Does Insulin Do? Retrieved from https://www.diabetesselfmanagement.com/blog/what-does-insulin-do/

Diabetes Prevalence. (2018). Retrieved from https://www.diabetes.co.uk/diabetes-prevalence.html

Dinsmoor, R. S. (2006, June 05). Beta-Cell Regeneration. Retrieved from https://www.diabetesselfmanagement.com/diabetes-resources/definitions/beta-cell-regeneration/

Gerber, P. A., & Rutter, G. A. (2017, April 01). The Role of Oxidative Stress and Hypoxia in Pancreatic Beta-Cell Dysfunction in Diabetes Mellitus. Retrieved from https://www.ncbi.nlm.ni h.gov/pmc/articles/PMC5372767/

Gupta, S. C., Patchva, S., & Aggarwal, B. B. (2012). Therapeutic Roles of Curcumin: Lessons Learned from Clinical Trials. *The AAPS Journal*, 15(1), 195-218. doi:10.1208/s12248-012-9432-8

Gutowski, M., & Kowalczyk, S. (2013, November 01). A study of free radical chemistry: Their role and pathophysiological significance. Retrieved from https://pdfs.semanticscholar.org/1539/7bc107cd8a2f0ae5fbd50e372da944c6b119.pdf

Jurenka, J. S. (2009). Anti-inflammatory Properties of Curcumin, a Major Constituent of Curcuma longa: A Review of Preclinical and Clinical Research. *Alternative Medicine Review*, 14(2), 141-153. Retrieved from http://archive.foundationalmedicinereview.com/publications/14/2/141.pdf

Kumar, S. S., Houreld, N., & Abrahamse, H. (2018). Therapeutic Potential and Recent Advances of Curcumin in the Treatment of Aging-Associated Diseases. *Molecules*, 23(4), 835. doi:10.3390/molecules23040835

Lee, J., Ma, K., Moulik, M., & Yechoor, V. (2018). Untimely oxidative stress in β-cells leads to diabetes – Role of circadian clock in β-cell function. *Free Radical Biology and Medicine*, 119, 69-74. doi:10.1016/j.freeradbiomed.2018.02.022

Lobo, V., Patil, A., Phatak, A., & Chandra, N. (2010). Free radicals, antioxidants and functional foods: Impact on human health. *Pharmacognosy reviews*, 4(8), 118-26.

Marrocco, I., Altieri, F., & Peluso, I. (2017). Measurement and Clinical Significance of Biomarkers of Oxidative Stress in Humans. *Oxidative Medicine and Cellular Longevity*, 2017, 1-32. doi:10.1155/2017/6501046

Menon, V. P., & Sudheer, A. R. (2007). Antioxidant And Anti-Inflammatory Properties Of Curcumin. ADVANCES IN EXPERIMENTAL MEDICINE AND BIOLOGY *The Molecular Targets and Therapeutic Uses of Curcumin in Health and Disease,* 105-125. doi:10.1007/978-0-387-46401-5_3

Modak, M. A., Parab, P. B., & Ghaskadbi, S. S. (2011). Control of hyperglycemia significantly improves oxidative stress profile of pancreatic islets. *Islets*, 3(5), 234-240. doi:10.4161/isl.3.5.15941

Moghadamtousi, S. Z., Kadir, H. A., Hassandarvish, P., Tajik, H., Abubakar, S., & Zandi, K. (2014). A Review on Antibacterial, Antiviral, and Antifungal Activity of Curcumin. *BioMed Research International*, 2014, 1-12. doi:10.1155/2014/186864

National Cancer Institute. (2018). Reactive Oxygen Species. Retrieved from https://www.cancer.gov/publications/dictionaries/cancer-terms/def/reactive-oxygen-species
National Institute of Diabetes and Digestive and Kidney Diseases (NIDDK). (1999). Bethesda, MD: National Institute of Diabetes and Digestive and Kidney Diseases, U.S. Department of Health and Human Services.
Newsholme, P., Haber, E. P., Hirabara, S. M., Rebelato, E. L., Procopio, J., Morgan, D., . . . Curi, R. (2007). Diabetes associated cell stress and dysfunction: Role of mitochondrial and non-mitochondrial ROS production and activity. *The Journal of Physiology*, 583(1), 9-24. doi:10.1113/jphysiol.2007.135871
Pancreatic Islet Transplantation. (2018, October 01). Retrieved from https://www.niddk.nih.gov/health-information/diabetes/overview/insulin-medicines-treatments/pancreatic-islet-transplantation
Qi, M., Barbaro, B., Wang, S., Wang, Y., Hansen, M., & Oberholzer, J. (2009). Human Pancreatic Islet Isolation: Part I: Digestion and Collection of Pancreatic Tissue. *Journal of Visualized Experiments*, (27). doi:10.3791/1125
Qi, M., Barbaro, B., Wang, S., Wang, Y., Hansen, M., & Oberholzer, J. (2009). Human Pancreatic Islet Isolation: Part II: Purification and Culture of Human Islets. Journal of Visualized Experiments, (27). doi:10.3791/1343
Rodrigo, R. (2009). Oxidative Stress and Antioxidants: Their Role in Human Disease. New York, NY: Nova Science.
Rojas, J., Bermudez, V., Palmar, J., Martínez, M., Olivar, L., Nava, M., . . . Velasco, M. (2018, February 19). Pancreatic Beta Cell Death: Novel Potential Mechanisms in Diabetes Therapy. Retrieved from https://www.hindawi.com/journals/jdr/2018/9601801/
Sano, T., Umeda, F., Hashimoto, T., Nawata, H., & Utsumi, H. (1998). Oxidative stress measurement by in vivo electron spin resonance spectroscopy in rats with streptozotocin-induced diabetes. *Diabetologia*, 41(11), 1355-1360. doi:10.1007/s001250051076
Uppu, R. M., Murthy, S. N., Pryor, W. A., & Parinandi, N. L. (2010). *Free radicals and antioxidant protocols*. New York, NY: Humana Press.
Williams, J., Jacus, N., Kavalackal, K., Danielson, K. K., Monson, R. S., Wang, Y., & Oberholzer, J. (2018). Over ten-year insulin independence following single allogeneic islet transplant without T-cell depleting antibody induction. *Islets*, 10(4), 168-174. doi:10.1080/19382014.2018.1451281
Wu, L. L., Chiou, C., Chang, P., & Wu, J. T. (2004). Urinary 8-OHdG: A marker of oxidative stress to DNA and a risk factor for cancer, atherosclerosis and diabetics. *Clinica Chimica Acta*, 339(1-2), 1-9. doi:10.1016/j.cccn.2003.09.010

APPENDIX

Graphs of Antioxidant Enzymes

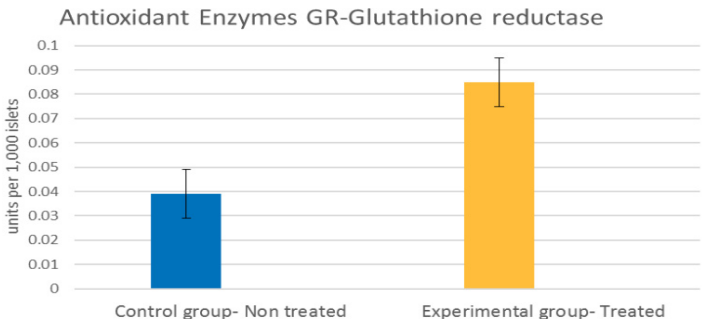

Figure 7.2. Antioxidant Enzyme GR - Glutathione Reductase

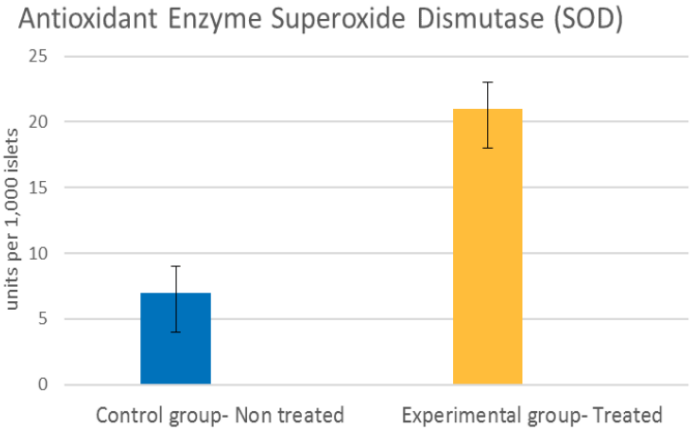

Figure 7.3. Antioxidant Enzyme Superoxide Dismutase (SOD)

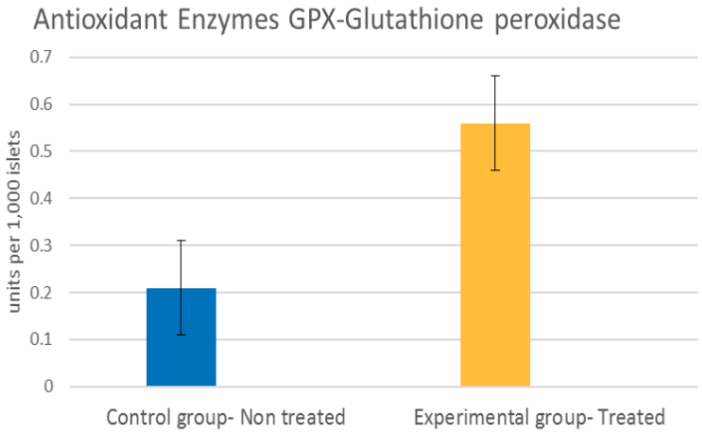

Figure 7.4. Antioxidant Enzyme GPX - Glutathione Peroxidase

Graphs of Antioxidant Molecule

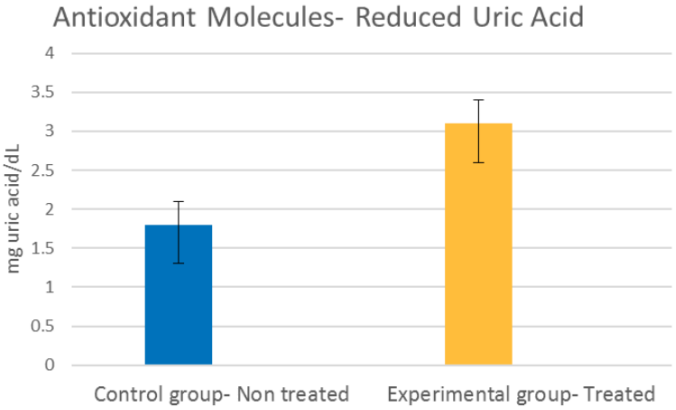

Figure 8.2. Antioxidant Molecule - Reduced Uric Acid

Data Analysis for Each Analysis Technique

Estimation of Lipid Peroxidation, Protein Carbonyl, and Amount of 8OHdG:

Estimation of Protein Carbonyls	Average	SD
Control group- Non treated	556	34
Experimental group- Treated	243	31

(Units: nmoles of protein carbonyls per mg protein)

Estimation of Lipid Peroxidation	Average	SD
Control group- Non treated	174	29
Experimental group- Treated	90	21

(Units: µmoles of MDA formed per 100 mg tissue)

Amount of 8OHdG in islet nuclear DNA	Average	SD
Control group- Non treated	40	12
Experimental group- Treated	10	15

(Units: mmoles per microgram/DNA)

Antioxidant Enzymes:

	Catalase		SOD	
Antioxidant Enzymes (Catalase and SOD)	Average	SD	Average	SD
Control group- Non treated	7	3	11	4
Experimental group- Treated	21	6	27	9

(Units: units per 1,000 islets)

Antioxidant Enzymes (GR-Glutathione reductase)	Average	SD
Control group- Non treated	0.039	0.01
Experimental group- Treated	0.085	0.01

(Units: units per 1,000 islets)

Antioxidant Enzymes (GPX-Glutathione peroxidase)	Average	SD
Control group- Non treated	0.21	0.07
Experimental group- Treated	0.56	0.05

(Units: units per 1,000 islets)

Antioxidant Molecules:

Antioxidant Molecules (Reduced Glutathione)	Average	SD
Control group- Non treated	48	16
Experimental group- Treated	95	11

(Units: nmoles of reduced glutathione/100 mg wet weight)

Antioxidant Molecules (Reduced Uric Acid)	Average	SD
Control group- Non treated	1.8	0.3
Experimental group- Treated	3.1	0.1

(Units:mg uric acid/dL)

Islet Viability Dosage Determination:

Dosage		
10uM	Control Group- non-treated	78
	Experimental Group- treated	80
20 uM	Control Group- non-treated	75
	Experimental Group- treated	95
40 uM	Control Group- non-treated	76
	Experimental Group- treated	90
80uM	Control Group- non-treated	77
	Experimental Group- treated	91

Units: Viability % by FDA/PI Stain

Islet Viability:

Pancreases	Control Group - non-treated	Experimental Group - treated
Pancreas #1	65	81
Pancreas #2	74	94
Pancreas #3	77	91
Pancreas #4	73	89
Pancreas #5	68	95
Pancreas #6	68	94
Pancreas #7	74	89
Pancreas #8	65	96
Pancreas #9	74	91
Pancreas #10	75	90

Units: Viability % (20uM)[n=10]

Islet Recovery:

Pancreases	Control Group - non-treated	Experimental Group - treated
Pancreas #1	68	81
Pancreas #2	71	92
Pancreas #3	78	91
Pancreas #4	71	89
Pancreas #5	68	92
Pancreas #6	71	94
Pancreas #7	74	89
Pancreas #8	65	94
Pancreas #9	74	91
Pancreas #10	74	94

Units: Recovery %

Insulin Secretion:

Low Glucose	Control Group - non-treated	Experimental Group - treated
Pancreas #1	15	25
Pancreas #2	18	28
Pancreas #3	12	24
Pancreas #4	10	18
Pancreas #5	21	29
Pancreas #6	16	26
Pancreas #7	17	25
Pancreas #8	21	29
Pancreas #9	11	24
Pancreas #10	12	25
High Glucose	**Control Group - non-treated**	**Experimental Group - treated**
Pancreas #1	31	74
Pancreas #2	38	79
Pancreas #3	41	86
Pancreas #4	30	45
Pancreas #5	51	98
Pancreas #6	42	87
Pancreas #7	45	83
Pancreas #8	52	101
Pancreas #9	55	99
Pancreas #10	59	111

Units: ulUnit/ml

Mouse Transplant:

	Before Transplant	Day 1	Day 2	Day 3	Day 4	Day 5	Day 6	Day 7	Day 14	Day 21	Day 30
Control Group - non-treated	530	428	398	388	375	365	359	349	240	200	180
Experimental Group - treated	547	225	169	178	178	159	111	134	128	112	113
Diabetic Control	467	469	460	455	427	409	450	437	451	423	417
Non-Diabetic Control	85	82	89	81	78	86	88	84	82	84	81

Units: mg/dL

Engineering an Automated Chloramine Testing Device

Anna Morgan[1]
[1]**duPont Manual High School**
Louisville, Kentucky

ABSTRACT

Most swimmers are familiar with the distinct chlorine smell that is often detected around an indoor pool. However, many are unaware that they are actually inhaling a dangerous compound called chloramine. When inhaled in high concentrations, chloramine is known to cause negative health effects, such as damage to the lung's Clara cell system, the natural defense to trace amounts of toxic gases. A correlation has also been shown between exposure to chloramines at a young age and the development of asthma later in life. However, despite these known health risks, most natatoriums are not equipped with dependable systems to remove chloramines from the air. The goal of this project was to create a device that could test and remove chloramines from the air of indoor pools while remaining cost-effective and practical for the setting. The device was designed to automate the DPD test, a system of testing which is traditionally performed by hand. An Arduino microcomputer executed this method, using an LED and photoresistor reading to test the color of the different solutions. The device was ultimately successful at meeting the engineering goal after several improvements and modifications. The device provides accurate readings of chloramine concentrations before sending a signal to a pool's HVAC systems to control an exhaust fan. Therefore, the device has been shown to be an effective product to mitigate the negative health effects caused by the inhalation of chloramines.

INTRODUCTION

Most swimmers and spectators are aware of the distinct smell associated with indoor pools, but many do not recognize the negative effects of the chemicals they are breathing. People commonly recognize this pool smell as chlorine, while what they are actually breathing in is a compound called chloramine. Chloramines are proven to have several negative health effects and can cause respiratory diseases. The effect of chloramines is a relatively unspoken topic amongst swimmers and spectators at indoor pools. Most participants are simply unaware of the issue and are instead gradually affected by the chemical until it results in serious health issues. The goal of this project was to build a device to remove chloramines from the air around the pool in a cost-effective manner based on the concentration of chloramines in the pool water.

Chloramines are created due to the chlorine that is put into pools for cleaning purposes. When ammonia emitted by humans through fluids such as urine or perspiration combines with the chlorine, chloramines are created (Centers for Disease Control and Prevention, 2016). The chloramines then evaporate into the air above the pool. However, because they are denser than other gases in the air, they settle in the low hanging air near the surface of the water, displacing oxygen. This means that when swimmers take breaths while swimming, they inhale concentrated chloramines instead of oxygen, which is harmful to the swimmers' health.

Most swimmers and spectators are familiar with the eye irritation, coughing, and wheezing that are associated with short-term exposure to chloramines. However, long-term exposure is linked to more lethal health problems. A study by Angela Spivey with the Environmental Health Perspectives (EHP) showed that children exposed to high concentrations of chloramines over a long period of time had significantly damaged Clara cell systems (2004). The main function of this system is to protect the bronchiolar epithelium in small pathways of lungs from harmful gases. The study showed that long-term exposure to chloramines lowered the body's production of a protein called CC16, which acts as a natural anti-inflammatory agent in the lungs. This production in the lungs is the body's natural defense to small concentrations of harmful gases such as ozone. Damage to this system at a young age can leave a swimmer susceptible

to harmful gases, even in adulthood. A study conducted by A. Bernard, S Carbonnelle, and several other authors showed a link between chloramine exposure and an increased risk for asthma in school children (2003). Although the study did not focus on the biological cause of this correlation, it did identify a pattern showing that the greater the amount of exposure to chloramines, the higher the likelihood of asthma developing later in childhood. This correlation could be caused by the weakening of the lungs after damage to the Clara cell system, which is described in Spivey's study.

The negative health effects of chloramines have led to the establishment of legal concentrations of chloramines that are allowed in public pools. This limit is .04 parts per million (ppm), which is when chloramines first become irritating to swimmers. As a general rule, when chloramines can be detected with scent, the concentration is likely higher than the legal limit. These laws exist to protect swimmers from the dangerous chemicals that they would otherwise regularly inhale. However, these laws are almost impossible to enforce as there is no common method of testing the concentrations of chloramines in the air. Even large pool chemistry companies do not have the resources to test for chloramines in the air on a regular basis. Indoor pool facilitators tend to ignore the harmful effects because the concentration cannot be proven, and this problem is commonly unknown to the general public. This makes the need for an affordable way to remove chloramines even greater, as pool owners are usually resistant to spending large amounts of money on removal systems.

There are some products developed by private companies to mitigate the effects of concentrated chloramines. However, most of them focus on filtering air from high areas and never reach the heavy chloramines that rest near the surface of the water. Other products attempt to blow the concentrated chloramines from the surface of the pool. This causes uncomfortable, cold drafts for swimmers and only spreads the chloramines throughout the rest of the room. One device developed by Paddock, called the Evacuator, is arguably the most effective system for removing chloramines from the air. This device is most similar to the goal of this project. The system is installed around the drainage system of pools and focuses on filtering out the air from the pool's surface and removing it from the entire facility. Even this design, however, is still flawed. The installation of the system can be incredibly expensive and requires reconfiguring much of the pool's drainage system. It is also problematic because when large amounts of air are constantly being removed from the space, new, clean air must be heated to the right temperature to replace it. Since chloramines are already an unpopular issue, most pool facilitators are not willing to spend extensive amounts of money to go through this process to solve the problem. Therefore, an affordable device needs to be created in order to filter the chloramines out of the air.

The goal of this project was to create a device to effectively remove chloramines from the air in an affordable manner. In order to cut the costs of operating the device, it does not need to run constantly. The amount of chloramines in the air is proven to be significantly higher when the pool is full of swimmers during a large swim meet, rather than at night when no one is in the pool. Therefore, the device can test the amount of chloramines and only filter out air when concentrated amounts are present. However, because there is no cost-effective way to test chloramines in the air, the measurements must be taken from the water, which yields a concentration proportionate to that of the air. This device is different from Paddock's product as it does not require the same lengthy and expensive installation. The device developed by the project is the only cost-effective and portable solution that can be used by indoor pools. This will hopefully lead to the more widespread use of chloramine removal equipment in order to mitigate the health effects.

The device also needed to be relatively portable and function in an indoor pool environment, meaning it needed to be waterproof and not take up an excessive amount of space. This purpose of the device is similar to the Evacuator because it is the most effective device currently available. In addition, this project addresses the flaws previously described in the Evacuator system. The device created is portable and does not require expensive installation to increase the availability of the product. The device also tests the concentration of chloramines in the water and only filters air when necessary in order to save money used from reheating replacement air, which is one of the main deterrents from the use of the system.

To prove the device's effectiveness, water

with different amounts of chloramine concentrations was tested by the machine to see if it begins to filter out air at each concentration. The device should begin filtering out air when the concentration rises above .4 ppm, which is the legal concentration of chloramines in the air. A successful device will meet all of the parameters described and have the ability to be mass-produced.

METHODOLOGY

The design for the construction of the device to complete the engineering goal of the project was created based on research and collaboration with experts in the field. This design was believed to achieve the goal in theory. However, the process was altered and improved after testing as necessary. The construction was completed in two basic parts: the mechanical portion and the coding portion.

The mechanical portion of the project was completed first, beginning with a 35 cm x 20 cm x .1 cm piece of simple plywood. Five circular holes with a diameter of 2 cm were then cut out of the wood with a jigsaw. They were 1 inch from the shorter end of the wood and evenly spaced horizontally. When operating the jigsaw, appropriate precautions were taken, such as wearing goggles and using adult supervision. Next, a 1 cm x 2 cm x 20 cm piece of plywood was attached to the lower end of the device (as shown in Figure 1) using hot glue in order to support the glass test tubes. The second piece of 1 cm x 2 cm x 10 cm plywood was attached 1 inch above the device and flushed to the left side of the device. The jigsaw was used to cut two circular holes with a 3 cm diameter through this piece of wood from the top through the bottom of the device. Test tubes were then able to be placed through these holes and rest on the bottom piece of plywood. Even with the top piece of plywood, a 1 cm x 2 cm x 10 cm block of plywood was flushed to the right of the device. After this step, the structure was complete and additional devices were attached to the structure.

Underneath the 1 cm x 2 cm x 10 cm block of plywood, an HYCC Laboratory Magnetic Stir Plate was placed so that the plastic tube rose up between the separation of the two pieces of plywood, as shown in Figure 1. Velcro strips were used to secure this stirrer so that it could be removed as desired. Five pumps were then placed through the holes and secured with hot glue so that the wiring faced the back of the device, and the front remained in front of the wood. On each pump, four screws were used to attach the plastic cover on the pumps. These screws were removed and set aside as the 3 mm of plastic tubing that was initially running through the pump was replaced with 2 mm plastic tubing. This decreased the flow rate of the pumps in order to allow for more precise emissions later in testing. Each 2 mm tube inserted was 80 cm in length before being cut later in the procedure. The plastic covers of the pumps were reattached using the screws used prior. Simple painter's tape was then used to label each pump going from left to right as P2, P4, P5, P6, and P1 in marker on the tap. These labels were useful in testing and construction but were later removed from the final product. Two 150 ml glass test tubes were then placed through the holes in the top piece of plywood so that they rested on the wood at the bottom of the device.

The front of the device was completed, and the wood was flipped to view the opposite side. An 8 module relay was placed directly below the five pumps using velcro tape so that the high voltage connections were directed towards the pumps and the lower voltage connections towards the opposite side, as shown in Figure 2. This allowed for less wiring to be used, creating a more simple device. Four 1.5 V battery connectors were then placed in series orientation to the left of the relay, as exact placement was not necessary. These battery connectors were attached to the device using velcro strips. Three simple breadboards were then placed and secured with velcro to the right of the battery and below the relay modules, as shown in Figure 2. An Arduino Uno Microcomputer was placed at the bottom right corner of the wood using velcro strips. This Arduino was attached to a 9V battery source through the power cable of the Arduino.

The wiring of the device was the next portion to be completed. The resulting wiring is displayed in Figure 2. Firstly, the water pumps must be attached to the battery connectors and appropriate relay modules. A soldering iron and metal were used to attach a solid 22 gauge copper wire with a red coating to each of the pumps. The wire was attached to the small metal rod on the back of each pump next to the "+" sign imprinted on the plastic backing. When using the soldering iron, proper safety measures, such as ventilation

and adult supervision, were taken. This process was repeated, attaching a solid 22 gauge copper wire with black coating to each of the other metal rods on the pumps. This color code helped ensure circuits flowed in the correct direction by differentiating the positive and negative directions. The opposite ends of each red wire were connected in series to the far left breadboard. Connected to the breadboard in this same series was a single jumper wire, which was attached to connect the circuit to the battery connector on the connector's negative side. A similar circuit was then created on the same breadboard but in a different series. A single jumper wire connected the series to the other side of the battery. The five wires that left this series went into the normally open connection in the corresponding relay. For example, the wire connecting pump three was connected to module three on the breadboard. The five black wires connected to the pumps were also attached to the ground compartment of the corresponding relay to close the circuit.

The connection between the Arduino and the relay was made using male to female jumper wires. The ten low voltage wires on the opposite end of the relays were used to connect each of the pumps to the Arduino. Relays 1-5 were connected to their corresponding pins on the Arduino, while relays 6-8 remained idle and unconnected. A female to male connector was also used to connect the VCC pin on the relay to the second breadboard. A 5V power source was placed in series of this pin to give the relay power. Another male to female wire was needed to attach the negative end of this powered circuit to the ground pin of the relay. An additional wire was run from the circuit to the GND pin of the Arduino.

On the front of the device, an Arduino Photoresistor was placed so that the sensor rested on the side of the testing chamber of the stirrer. The wires of the photoresistor went through the two small holes drilled into the device, leading to the back wiring. The same was completed with a white LED light on the opposite side of the chamber, also leading to the back of the device. These wires were connected to female to male jumper wires on the back of the device so that all wires have male endings to complete connections. The longer, positive wire leading from the LED was placed in pin 8 of the Arduino. Meanwhile, the negative wire was connected to another GND pin. Each wire of the photoresistor is connected to the third and final breadboard. To complete this circuit, a wire was lead from the breadboard to the A0 pin on the Arduino, and another was lead to a GND pin. A 100 Ohm resistor was also used in the circuit to lower the voltage.

The next section of the project completed was the coding portion. The code was written on the Arduino Code Creator program and then uploaded to the Arduino through USB. The code was written to allow the device to automate the DPD test for free and total chlorine. First, pump 3 was run for ten seconds, or 10000 milliseconds, to allow 250 ml of the pool water to flow into the testing chamber. Next, pump 1 was allowed to run for 250 milliseconds, adding DPD 1A to the testing chamber. Pump 2 was then allowed to run for 250 milliseconds to add DPD 1B to the mixing chamber. A delay was then entered into the program for 10000 milliseconds to allow the magnetic stirrer to mix the solution completely. The LED is then turned on high, and a 1000 millisecond delay was added before the photoresistor takes its reading. Another 1000 millisecond delay was written into the program before turning the LED off. The value of resistance was then recorded by the photoresistor and stored in a variable. If-then statements were used to convert the value to a ppm calculation of free chlorine based on the calibration from liquid with known calculations.

The procedure to test for total chlorine was added into the program, beginning with turning on pump 3 for 250 milliseconds to add DPD 3 to the solution. A 100000-millisecond delay was written into the program to allow the stirrer to fully incorporate the reagent. The LED was then turned on, followed by a 1000 millisecond delay before the photoresistor took another reading. This reading was stored into a variable for total chlorine, and after a 1000 millisecond delay, the LED was turned off. The program converted the photoresistor reading to a ppm value as it was completed for the free chlorine test. The calculation portion of the code was then written by declaring a variable for the concentration of chloramines and initializing it as the concentration of total chlorine subtracted by the concentration of free chlorine. An if-then statement was written so that if the calculation was above the legal concentration of 4 ppm, a signal would be sent to the HVAC system. A 600000-millisecond delay

was then written to delay the rest of the procedure 1 hour before performing the test again.

Code was then written to drain and flush the mixing chamber. First, pump 4 was turned on, and a 25000-millisecond delay was added to drain the existing mixture. Pump 5 was then turned on before a delay of 25000 milliseconds to flush the testing chamber and prime the pump before the next test. Pump 5 was turned off, and a delay of 25000 milliseconds was written into the program before turning off Pump 4. This code was then verified by the Arduino to check for errors. If errors were found, the program was edited until acceptable. Finally, the program was compiled and uploaded to the Arduino Uno.

The initial design and instructions for the device's construction were created based on research and input from experts in the field. The procedures were meant to create a device that would fulfill the engineering goal of the project. Nevertheless, these procedures may be altered and improved based on trial and error during the testing of the device at different stages of the engineering process.

RESULTS

After all the data from the participants was collected, it was compiled into a table and multiple graphs.

Figure 1. Front Side of the Device

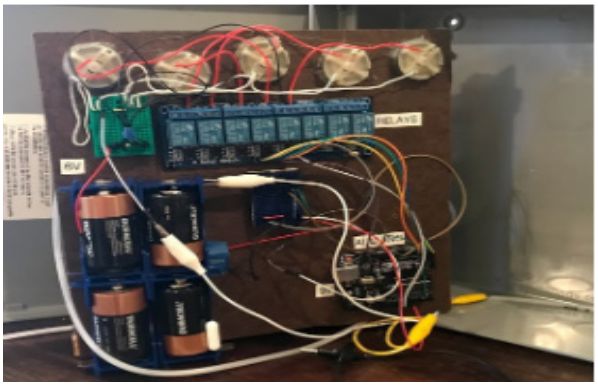

Figure 2. Back of the Device, Showing Electrical Components

Figures 1 and 2 show the final design of the device after all modifications were complete. After conferring with two mechanical engineers, Jarvis Head and Brent Falcone, as well as computer software engineer Billy Gardner, this design was determined to be the most efficient of those developed in the project. It was also confirmed by all three to meet the requirements specified in the engineering goal.

	Blair-wood Trial 1	Blair-wood Trial 2	Drury Inn Trail 1	Drury Inn Trial 2	Hyatt Trial 1	Hyatt Trial 2	Hotel Trail 1	Hotel Trail 2	Tap Trial 1	Tap Trial 2
Free Chlorine	2 ppm	2 ppm	0.75 ppm	0.75 ppm	1 ppm	1 ppm	0 ppm	0 ppm	0 ppm	0 ppm
Total Chlorine	4 ppm	4 ppm	1 ppm	1 ppm	2 ppm	2 ppm	0.5 ppm	0.5 ppm	2 ppm	2 ppm
Chloramines	2 ppm	2 ppm	0.25 ppm	0.25 ppm	1 ppm	1 ppm	0.5 ppm	0.5 ppm	2 ppm	2 ppm
Free Chlorine Color Reading	116 Ohms	123 Ohms	129 Ohms	130 Ohms	110 Ohms	123 Ohms	169 Ohms	165 Ohms	170 Ohms	167 Ohms
Total Chlorine Color Reading	76 Ohms	81 Ohms	123 Ohms	122 Ohms	121 Ohms	96 Ohms	150 Ohms	148 Ohms	118 Ohms	118 Ohms
Difference	40 Ohms	42 Ohms	6 Ohms	8 Ohms	-10 Ohms	27 Ohms	19 Ohms	17 Ohms	52 Olhms	49 Ohms

Table 1. Results of Pool Samples

Table 1 shows the concentration of chloramines of ten samples taken from 5 different pools, measured by test strips compared to measurements made by the device. This allowed for a comparison between the two in order to calibrate the device and test its accuracy. The readings in ppm are those of the test strips. The calculated chloramines are shown below the free and total chlorine calculations. The photoresistor readings are shown below those of the test strips, measured in ohms. While the program was altered to display this reading during testing, the final product converted

this to a ppm reading of chloramines and then only output whether or not the exhaust fan should be turned on.

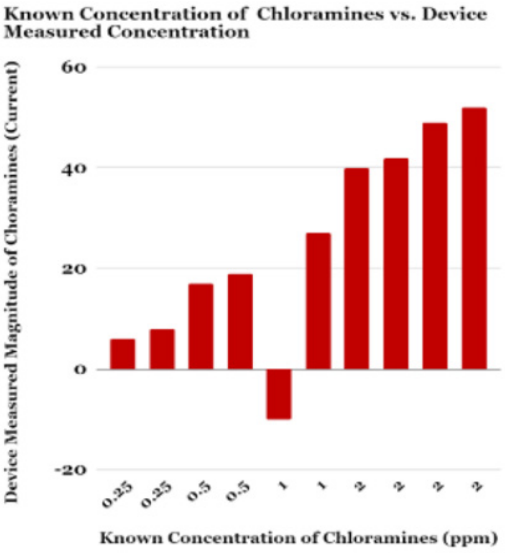

Figure 3. Graph of Device vs. Test Strips Results

Figure 3 shows the known concentration of chloramines in sampled water compared to the calculated magnitude of the chloramines by the device, showing that the device's measurement increases as the known concentration increases. However, there are some deviations from this pattern. For example, the first trial with 1 ppm of chloramines showed a negative magnitude of chloramines. The device measured this sample as having more free chlorine than total chlorine, which is impossible by definition. This resulted in an incorrect signal being submitted to the HVAC system.

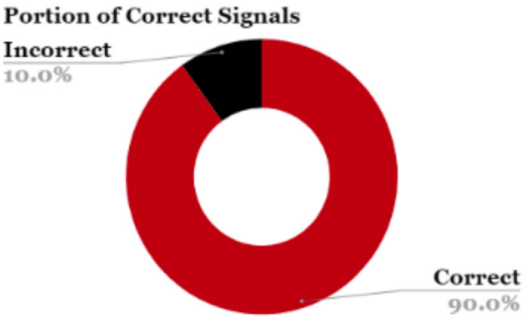

Figure 4. Graph of Portion of Correct Signals

Figure 4 displays, based on the calculations given, exactly what proportion of the signals sent to the HVAC system were consistent with the determination based on the test strips. 90% of the time, the correct signal was sent. Assuming the results follow a normal distribution, a sample confidence interval for p was calculated. It was determined with 90% confidence that the true proportion of signals sent by the device that are correct is between .7444 and 1.0. This calculation is based on the sample above, where 90% of signals aligned with known concentrations.

CONCLUSION

Testing of the final device throughout the project revealed that it meets the requirements defined by the engineering goal, ultimately creating a successful project. This goal, however, was only met after several modifications in the trial and error process. The initial design of the device was changed almost completely through the course of the project to meet the goal. Although many of these other designs may have been sufficient, the design chosen was determined to be the most practical to meet the engineering goal with the given resources.

In the initial stages of this project, the design of the device was simply a modification of the Paddock Evacuator system. The design added a testing chamber to the bench system so that it would only ventilate air when necessary to save natatoriums money so that more could afford the system. However, this design was met with several problems. Creating an effective way to ventilate air from an entire natatorium from a single device near the pool's edge would be difficult and expensive. In addition, adding electronics to the existing system would require a water-tight system so that no pool water could interfere with the electronics. This would be difficult because samples of the water must be used near the electronic to read sample concentrations.

After further research, the bench design was abandoned in favor of a device that would be placed in the pump room of an indoor pool, periodically sampling the water as it passes through the room. This design used two separate mixing chambers to test free and total chlorine and also did not include a magnetic mixer. The device also only used three pumps, draining the containers with solenoid valves instead. However, after conferring with mechanical engineer Jarvis Head, as well as Vice President of Ware Industries Brent Falcone,

this design was refined again. Falcone highlighted that the complicated connections between the testing chambers and the solenoid valves would make the color readings in the mixing chambers less consistent. Therefore, the design was altered to include two additional pumps to drain each chamber. This made it possible to use glass test tubes to mix the substances because they no longer required a connection to the solenoid valve below. The glass provides more accurate readings from the photoresistor because light can more easily pass through the glass than the plastic in the previous design. Falcon also recommended the use of peristaltic pumps to transport more precise volumes of liquid.

After further research, the design was again altered based on the finding that both free chlorine and total chlorine could be tested in a single solution. This alteration would eliminate inconsistencies and make the free chlorine and total chlorine tests more dependable by having them both make use of the same equipment. However, this change created the need for some sort of mixing device because a small amount of reagent must be added to a larger sample of water. Therefore, the test tube mixing chamber was replaced with a plastic tube above an electric mixer that remains on during the entire test of the device. The DPD testing method also requires an additional reagent. Therefore, one of the pumps previously used to drain the second testing chamber was converted to transport the third reagent.

These major changes lead to the final design of the device that completed the engineering goal. The device automates the DPD test, which tests chloramines by adding reagents to samples of pool water and then matching the color to a list of known concentrations. The level of free chlorine is then subtracted from that of the total chlorine. By automating this system, the device meets the requirement of accurately testing chloramines consistently. The device also sends a signal to a natatorium's HVAC system when the concentrations reach unsafe levels, meeting the requirement of removing the chloramines when necessary. The device is portable and inexpensive, fulfilling the requirements of the engineering goal.

Part of demonstrating the effectiveness of the device was proving that the reading of the concentration of chloramines in the water could be converted to a concentration in the air. In order to do this, the research was compared to that of Haugen. In Haugen's paper, Chlorine & Chloramine Testing - Lynnwood Recreation Center, he found a constant factor between the number of chloramines in the water of the pool and the number of chloramines in the air. However, this constant varies between pools because of differing sizes, ventilation systems, and other factors (2012). Nevertheless, after this constant is determined with calibration at each pool, the device could prove to be applicable and effective at each pool. With this study in mind, the device was tested, and the results were analyzed.

The data showed that the magnitude of chloramines measured by the device increased as the known concentration of chloramines in the water increased, implying that the device is capable of accurately measuring the concentration of chloramines in the water. Therefore, it is also capable of sending accurate signals to HVAC systems. Still, samples did deviate from this trend. For example, the first trial of water from the pool at the Hyatt Hotel suggested that the concentration of free chlorine was greater than that of total chlorine, which is both inconsistent with the test strip results and impossible by definition. This deviation from the pattern suggests inconsistencies in testing. This could be caused by the movement of the photoresistor in between testing or the movement of the electric mixer while testing. These inconsistencies could be mitigated through improvements to the device.

For example, testing how the photoresistor readings were affected by the movement of the magnetic stir plate revealed that readings were less consistent when the mixer remained on during testing. When the photoresistor was programmed to take continuous readings of a solution at constant color with the mixer on, readings within a range of 20 units were observed. Meanwhile, when the mixer was momentarily turned off while the photoresistor took several readings of the color of the solution again, the range shrank to about 10 units. This proves that turning the stirrer on and off during the testing process would be more accurate. This improvement could be achieved by connecting the stirrer's power source to a relay and the Arduino and then coding the Arduino to turn the stirrer on and off periodically during the testing procedure.

The device could also be made more accurate through running calibration with more samples at

different concentrations. The device is calibrated by performing tests on solutions with a known concentration of chloramines, which can be found with test strips. The photoresistor reading is then recorded; once a similar reading is calculated by the device, the concentration of that sample can be defined. The more samples that are used to calibrate the device, the more accurate its measurements will become.

Although these modifications to the device may help it become more accurate, they are not necessary for a successful project. The final device still meets the requirements of the engineering goal and functions as an effective prototype for a device that could be implemented into ventilation systems of natatoriums.

Angela Spivey and other researchers in this field have called for improved methods to minimize exposure to chloramines and similar chemicals. The purpose of this project was to combat many of these negative health effects posed by chloramines, which it was ultimately successful in doing. By improving and subsequently implementing the device, it can prove to be an effective means of mitigating the negative effects of chloramines.

REFERENCES

Activated Carbon Filter. (n.d.). Retrieved October 25, 2018, from https://askjan.org/products/Activated-Carbon-Filter.cfm

Brenard, A., Carbonnelle, S., Michel, O., Higuet, S., De Burbure, C., Buchet, J., . . . Doyle, I. (2003). Lung hyperpermeability and asthma prevalence in schoolchildren: unexpected associations with the attendance at indoor chlorinated swimming pools. Retrieved August 27, 2017, from http://oem.bmj.com/content/oemed/60/6/394.full.pdf

Centers for Disease Control and Prevention. (2016, May 4). Chemical Irritation of the Eyes and Lungs. Retrieved from https://www.cdc.gov/healthywater/swimming/swimmers/rwi/chemical-irritants.htmlDrinking Water. (2015, January 20). Retrieved August 30, 2017, from https://www.cdc.gov/healthywater/drinking/public/chloramine-disinfection.html

Fact sheets - Controlling chloramines in indoor swimming pools. (n.d.). Retrieved August 30, 2017, from http://www.health.nsw.gov.au/environment/factsheets/Pages/chloramines.aspx

Haugen , B. (2012, December 10). 2012 Chlorine & chloramine testing - lynnwood recreation center . Retrieved August 31, 2017, from file:///C:/Users/AMORG01/AppData/Local/Microsoft/Windows/INetCache/IE/115EDH77/2012%20Chlorine%20&%20Chloramine%20Testing,%20121012%20by%20ARCH%20Consulting%20Group.pdf

Healthy Swimming. (2016, May 04). Retrieved August 30, 2017, from https://www.cdc.gov/healthywater/swimming/aquatics-professionals/chloramines.html

Source Capture. (n.d.). Retrieved October 25,2018, from http://paddockevacuator.com/why-we-do-it/source-capture/

Spivey, A. (2004, December). Swimmer's Lung?: Indoor Pools and Respiratory Effects. Retrieved August 27, 2017, from https://www.ncbi.nlm.nih.gov/pmc/articles/PMC1331998/

The World Air Quality Index project. (n.d.). Sensing the Air Quality: Research on Air Quality Sensors. Retrieved September 05, 2017, from http://aqicn.org/sensor

Toxic Substances Portal - Chlorine. (2014, October 21). Retrieved September 05, 2017, from https://www.atsdr.cdc.gov/mmg/mmg.asp?id=198&tid=36